INT. J. REMOTE SENSING, 1991, VOL. 12, NO. 5, 877–920

Time-cumulated visible and infrared radiance histograms used as descriptors of surface and cloud variations

GENEVIEVE SÈZE

Laboratoire de Météorologie Dynamique du CNRS, 91128 Palaiseau Cedex, France

and WILLIAM B. ROSSOW

NASA Goddard Space Flight Center, Institute for Space Studies, New York 10025, U.S.A.

(Received 14 June 1989; in final form 15 January 1990)

Abstract. The spatial and temporal stability of the distributions of satellite-measured visible and infrared radiances, caused by variations in clouds and surfaces, are investigated using bidimensional and monodimensional histograms and time-composite images. Similar analysis of the histograms of the original and time-composite images provides separation of the contributions of the space and time variations to the total variations. The variability of both the surfaces and clouds is found to be larger at scales much larger than the minimum resolved by satellite imagery. This study shows that the shapes of these histograms are distinctive characteristics of the different climate regimes and that particular attributes of these histograms can be related to several general, though not universal, properties of clouds and surface variations at regional and synoptic scales. There are also significant exceptions to these relationships in particular climate regimes. The characteristics of these radiance histograms provide a stable well defined descriptor of the cloud and surface properties.

1. Introduction

Meteorological satellites allow for quasi-continuous observations of clouds over the whole globe and provide an opportunity to study the behaviour of clouds on space and time scales that are inaccessible from ground-based and aircraft data. Large regional or complete global coverage also provides better comprehension of the cloud characteristics associated with different climate (or dynamic) regimes (Hartmann and Short 1980, Cahalan *et al.* 1982, Minnis and Harrison 1984, Stowe *et al.* 1989, Rossow *et al.* 1989 b). Satellites can also observe cloud variations on a much wider range of space and time scales than available in other data, from about 10 m to planetary scale and about 30 min to many years. Previous studies have examined the mean properties of clouds and their regional and seasonal variations (Hughes and Henderson-Sellers 1985, Stowe *et al.* 1989, Rossow *et al.* 1989 b, Wylie and Menzel 1989); see Hughes (1984) for a historical review of ground-based cloud climatologies, diurnal and daily variations at spatial scales larger than 2·5° to 5° (Hartmann and Short 1980, Cahalan *et al.* 1982, Minnis and Harrison 1984, Hartmann and Recker 1986, Duvel 1988), and some aspects of longer-term variability (Short and Cahalan 1983). However, these more systematic studies have not

addressed cloud variability at smaller spatial scales (see case studies by Coakley and Bretherton 1982 and Welch *et al.* 1988) and at time scales from 1–20 days, where changes may be as significant and may also be an important aspect of the radiative properties of clouds (Cahalan *et al.* 1982). In addition, smaller scale radiance variations at different wavelengths are often not linearly correlated (Coakley and Baldwin 1984), suggesting that variations of cloud cover alone cannot provide a complete explanation of the cloud effects on radiation. Interpretation of satellite measured radiances in terms of other cloud physical properties is not straightforward (Rossow 1989).

A systematic survey of the complete range of space/time variations of satellite-measured radiances has not been done; thus, the key descriptors of the main cloud properties associated with different climate regimes have yet to be identified. Some studies have used the shape of the bidimensional radiance histograms to describe the radiance spatial distribution and classify cloud types (Desbois *et al.* 1982, Simmer *et al.* 1982, Platt 1983, Phulpin *et al.* 1983, Arking and Childs 1985). Desbois and Sèze (1984 a) also examined the time variations of these histograms. The underlying assumption in the techniques that use histograms to identify cloud types is that characteristic shapes are always related to the presence of specific cloud types; however, few of these methods have been tested on a comprehensive set of climate regimes.

The aim of this study is to test the space/time stability of the radiance histogram shapes in various climate regimes to determine their value as descriptors of cloud and surface behaviour over a fuller range of space and time scales. We focus on understanding the nature of cloud and surface variations associated with different climate regimes and not on the definition of a cloud classification algorithm. Moreover, we do not complete a survey of larger time scales, but rather investigate ways to describe the smaller scale behaviour more completely for use in such surveys. A companion paper (Sèze and Rossow 1991, henceforth SR91) describes the effect on these statistics produced by variations of data resollution, especially the effect of the data sampling performed by the International Satellite Cloud Climatology Project (Schiffer and Rossow 1983, 1985). Here, we use full resolution METEOSAT data which provides a complete sample of climate regimes with the exception of the polar regions. The spatial scales covered by these data range from about 5 to over 4000 km. We neglect diurnal variations and examine time variations over scales from 1 day to about 20 days; we briefly examine seasonal differences by comparing results from a summer and winter month.

The method of analysis of the radiance variations is described; in addition to the radiance histograms, we calculate a number of other statistical quantities from the histograms to determine the specific attributes of cloud and surface space/time variability that produce these histogram shapes. We present the radiance histograms and describe how they characterize the variations of clouds and surfaces that define each climate regime.

The effects of varying the time scale for cumulating the histograms are discussed and we examine the magnitude of time variations over a range of time scales from 1 to 20 days. We consider the effects of varying the spatial scale for cumulating the histograms and examine the magnitude of space variations over a range of scales from 5 to 1000 km. The relative contributions of time and space variations are then examined by comparing the same set of bidimensional histograms and other statistics calculated for time-composite images with those from the original images.

The time-composite images are formed by calculating specific statistics of the time series of radiances for each geographical location (e.g. the mode or the extrema of the distribution).

2. The data

The full resolution data used for this study are METEOSAT images from 15 July to 10 August 1983; all images are from 12.00 UT to maximize visible radiances and minimize sun-angle effects. The resolution of all radiance measurements is 5 km at the subsatellite point (the original 2·5 km resolution of the visible measurements is sampled to 5 km). The visible (VIS) measurements are made at an effective wavelength of 0·7 μm with a radiometric resolution of 64 levels (counts), which is equivalent to a precision of 2 per cent. The infrared (IR) measurements are made at 11 μm with 256 levels (counts), which is equivalent to a precision of 0·4 K in brightness temperature for the warmest desert regions, decreasing to about 0·5 K at brightness temperatures of 270 K and to 1 K for the highest (coldest) clouds. Because the atmosphere is nearly transparent at these two wavelengths, the distribution of VIS and IR radiances is produced primarily by the space and time variations of clouds and the surface (ocean or land).

METEOSAT is a geosynchronous weather satellite operated by the European Space Agency (ESA) that provides observations covering a region $\pm 70°$ of geocentric angle centred on the equator and the Greenwich meridian (figures 1 and 3), encompassing all of Europe and Africa, plus a portion of Brazil, and most of the North and South Atlantic Ocean. ESA re-maps these observations on to a fixed grid by simulating a geosynchronous satellite situated at a fixed position (the real satellite moves with time around this fixed position). Therefore, one scene element (or pixel) corresponds to one fixed geographical location.

Seven regions have been specially studied. They were chosen to represent the main types of radiance distributions observed from METEOSAT (figures 1 and 3): (1) North Africa (32° N, 6° E), (2) Sahel (19° N, 4° W), (3) south Sub-tropical Atlantic (16° S, 6° E), (4) tropical Atlantic (9° N, 20° W), (5) central tropical Africa (6° N, 27° E), (6) Europe (49° N, 13° E), and (7) North Atlantic (52° N, 21° W). These regions will be referred to as N. Africa, Sahel, S. Atlantic, Tr. Atlantic, Tr. Africa, Europe, and N. Atlantic†. We will sometimes refer to Tr. Atlantic and Tr. Africa, together, as the intertropical convergence zone (ITCZ). The size of these regions is (120 × 240) pixels, which corresponds to 5° in latitude and 10° in longitude at the subsatellite point. Bidimensional radiance histograms are constructed for four region sizes: (60 × 60) pixels (2·5 × 2·5°), (60 × 120) pixels (2·5° × 5°), (90 × 180) pixels (3·75° × 7·5°), and (120 × 240) pixels (5° × 10°), centred on these locations. All of these histograms are made for each day (single image) and accumulated over 2, 3, 4, ..., up to 17 or 20 days. Most of the results discussed are for regions with 60 × 120 pixels.

All of the statistics reported here are computed using VIS radiances with 64 levels, equivalent to about 2 per cent precision, and a reduced IR radiance resolution of 128 levels, equivalent to about 1 K precision. (We explore the effects of differing radiance resolutions in SR91). In the figures and tables presented, these

† Seventeen days of data were available for Sahel, S. Atlantic, Tr. Africa and Tr. Atlantic; 20 days of data were available for N. Africa, Europe and N. Atlantic.

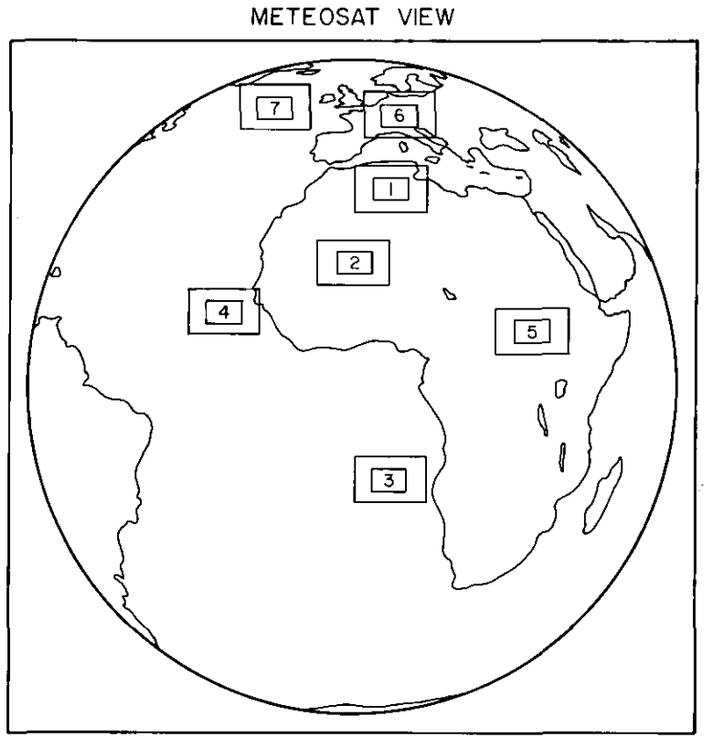

Figure 1. Geographic coverage provided by METEOSAT images. Special regions for this study are indicated by the rectangles, which show two of the four region sizes (referred to as 60 × 120 pixels and 120 × 240 in size in the text) used to determine the dependence of radiance statistics on spatial scale. Names used in the text to refer to these special study regions are (1) N. Africa, (2) Sahel, (3) S. Atlantic, (4) Tr. Atlantic, (5) Tr. Africa, (6) Europe, and (7) N. Atlantic.

radiances are rescaled to values from 0 to 255. This means that changes in VIS and IR, produced by changes in clouds and the surface and expressed in these count values, represent roughly the same magnitude changes in total radiation (i.e. a few watts per square metre). The IR scale has been reversed, therefore small counts in all tables and figures represent the highest brightness temperatures and large counts the lowest. Later in the discussion, when we refer to the minimum/maximum infrared radiances (IR MIN/MAX), this refers to the lowest/highest temperatures, not to the minimum/maximum count values. To avoid confusing radiances in the two spectral bands, we will refer to the lowest/highest VIS as darkest/brightest and the lowest/highest IR as coldest/warmest.

3. Method of analysis

Bidimensional histograms are formed by counting the frequency of occurrence of every pair of VIS and IR radiances (frequency is reported as a percentage of the total number of samples present). These histograms represent the variation of the VIS and IR spectral characteristics of clouds and the surface (1) in the spatial

domain (daily histograms from one satellite image, see figure 6; Desbois *et al.* (1982), Desbois and Sèze (1984a), Platt (1983)), (2) in the time domain (histograms of spatially averaged radiances: Hartmann and Short (1980), Hartmann and Recker (1986)), or (3) in both the space and time domains (timed cumulated histograms, see figure 4; Sèze and Desbois (1987)).

We describe these bidimensional histograms using properties of associated VIS and IR monodimensional radiance distributions (see figure 5), their mutual correlation (COR), and several other statistical quantities (table 1): minimum (MIN), maximum (MAX), average (AVG), mode (MOD), mode frequency (PEAK), and the standard deviation (SD). These quantities are calculated for the one-dimensional (1D) VIS and IR distributions. The MOD and PEAK are also computed for the 2D distribution, indicated by the prefix, VIS–IR, or by the suffix, 2. All of these quantities are computed for the 17 day (or 20 day) time-cumulated histograms (called CUM parameters), for each set of histograms accumulated for N days (N varying from 2 to 19), called CUMN parameters, and for each daily histogram to show their evolution with time. The average and standard deviation of the daily values (called AVG parameters and SD parameters), are also calculated. All of the short labels used to represent these quantities in this paper are summarized in table 1.

One quantitative measure of radiance variation or histogram dispersion is the percentage of the total possible radiances occurring in each histogram; this percentage is called CUM-AREA, referring to the 'surface area' of the histogram. To define the high-frequency part(s) in each bidimensional histogram, we calculate the area inside isolines defined by a frequency chosen such that the portion of the population inside the isolines is, for example, 80 per cent, and the portion outside is 20 per cent (radiances inside the isoline have a higher frequency than radiances outside). To determine these isolines, the cumulative fraction of the total population as a function of the frequency is calculated (figure 2 shows the results for the seven study regions). These curves give an indication of the overall compactness of the radiance

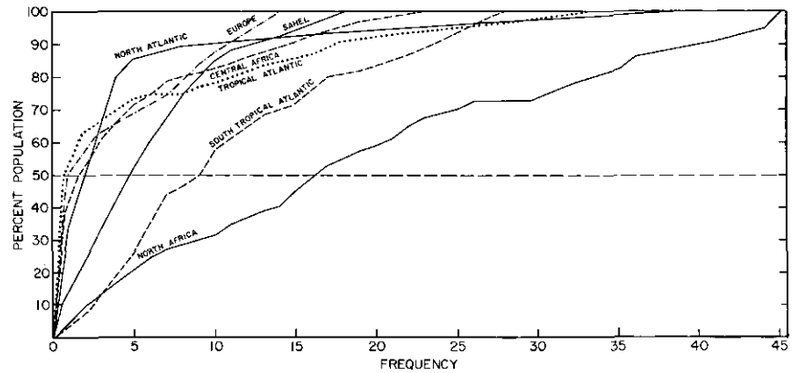

Figure 2. Cumulative frequency distributions for the bidimensional histograms, collected in 60 × 120 pixel regions over 17 days, six of which are shown in figure 4. The curves show the fraction of the total histogram population with frequencies below the value shown on the abscissa. Frequencies are expressed as a fraction of the total population in the histogram in increments of 0·1 per cent. The horizontal dashed line indicates the frequency value that corresponds to the innermost contour in figure 4.

distribution and also of the 'sharpness' of the distribution around the mode value. The 80 per cent isoline is the intermediate contour in figures 4 and 6 and the inner contour in figure 4 is the 50 per cent isoline. The fractions of the total possible surface area contained inside the 80 per cent isolines and 50 per cent isolines are called 80 per cent CUM-AREA and 50 per cent CUM-AREA.

The variation of radiances on larger spatial scales is evaluated by examining the changes in the histogram statistics as the size of the cumulating region is changed from about 350 to 1200 km across. We also examine the changes in histogram shape at scales up to about 1000 km. For the smaller spatial scales (5 to 350 km), the distribution of radiance differences is calculated between pairs of image pixels separated by N pixels. The time-scale dependence is examined from the variation of

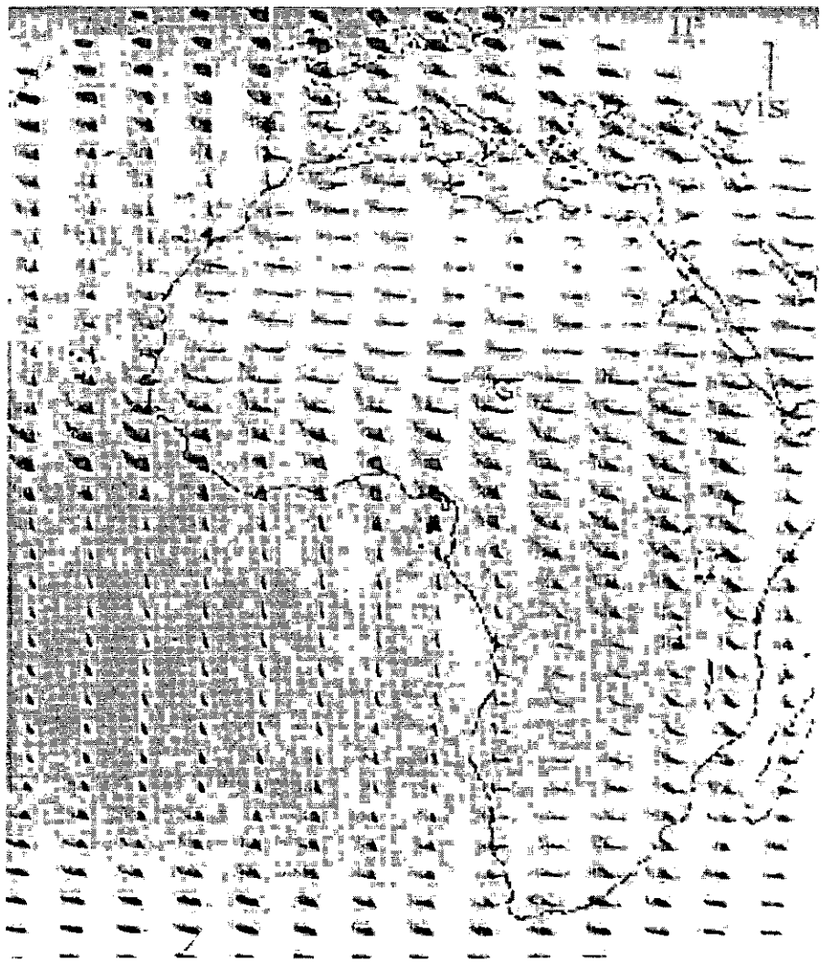

(*a*)

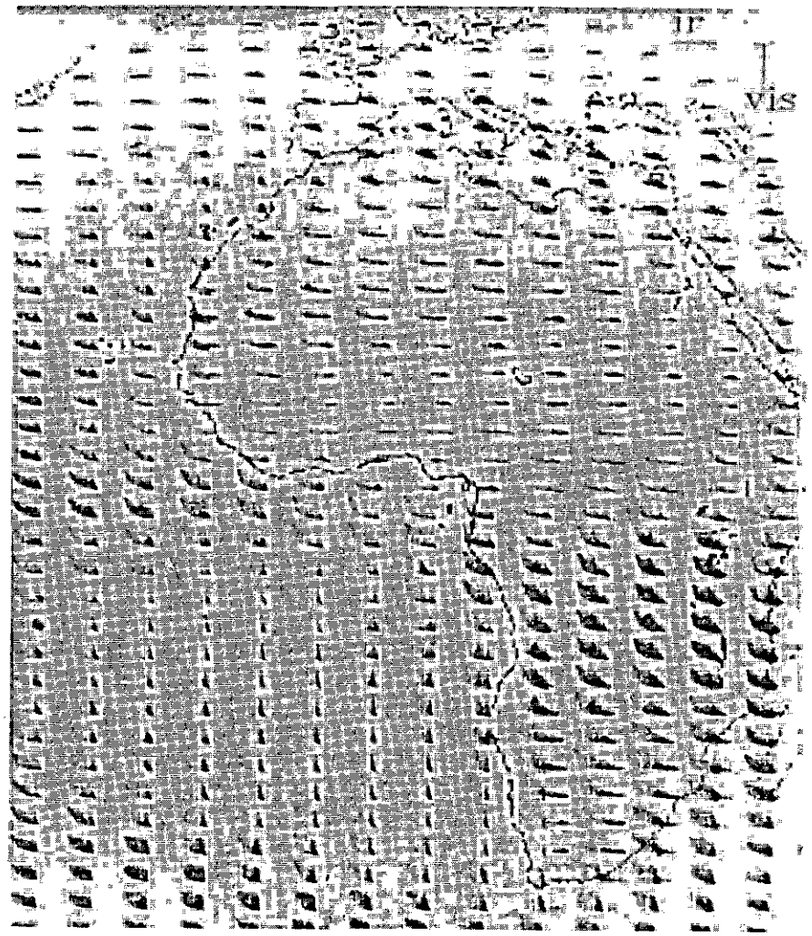

(*b*)

Figure 3. Radiance histogram shapes for the entire METEOSAT region for (*a*) July 1983 and (*b*) January 1984. Each histogram is formed by cumulation over regions of 60×120 pixels and over the whole month, using the sampled data (SR91). Visible radiances are displayed in the vertical direction (dark at bottom) and infrared in the horizontal direction (warm to the right).

the histogram statistics with the length of the cumulation time period from 1 to 20 days. Smaller time-scale variations are examined by calculating the radiance differences between pairs of pixels at the same location separated by N days.

Another way to illustrate the separate contributions of time and space variations is to examine the spatial variations of the time-series statistics at each location; this is done by calculating all of the same histograms and associated statistics of 'time-composite' images. In these images, the value associated with a scene element is a

Table 1. Definitions of symbols used to represent various statistical quantities calculated from the monodimensional and bidimensional visible (VIS) and infrared (IR) radiance distributions cumulated over various time and space scales.

VIS	visible radiance values (0·7 μm) as counts from 0–255, representing small to large values with a precision of 2 per cent.
IR	infrared radiance values (11 μm) as counts from 0–255, representing large to small values with a precision of 1°C near 20°C.
Statistics computed from monodimensional radiance distributions	
(VIS/IR means VIS and/or IR, also indicated by suffix of 1)	
VIS/IR MIN	minimum, darkest/coldest, radiances
VIS/IR MAX	maximum, brightest/warmest, radiances
VIS/IR AVG	average radiances
VIS/IR SD	standard deviation of radiances
VIS/IR MOD	most frequent radiance value (mode)
VIS/IR PEAK	largest frequency in the histogram, expressed as a fraction of the total image pixel population
r.m.s.	root mean square of radiance differences between any pair of image pixels in the distribution
Statistics computed from bidimensional radiance distributions	
(VIS-IR means VIS and IR, also indicated by a suffix of 2)	
VIS/IR MOD	most frequent pair of radiance values (mode), not generally equal to individual MOD1 values
VIS-IR PEAK	largest frequency in the histogram, expressed as a fraction of the total image pixel population
VIS-IR COR	correlation between the VIS and IR values
AREA	area occupied by the bidimensional histogram as a percentage of the total possible area in the VIS–IR space
80 per cent isolines	frequency isolines in the bidimensional histogram defined by the frequency chosen such that the portion of the population inside the isolines is 80 per cent and the portion outside is 20 per cent; radiances inside the isoline have a higher frequency than radiances outside
80 per cent AREA	area occupied by the higher frequency portion of the bidimensional histogram and defined by the 80 per cent isolines
50 per cent isolines	frequency isolines in the bidimensional histogram defined by the frequency chosen such that the portion of the population inside the isolines is 50 per cent and the portion outside is 50 per cent; radiances inside the isoline have a higher frequency than radiances outside
50 per cent AREA	area defined by the 50 per cent isolines
Cumulation statistics	
CUM parameters	prefix for quantities obtained from histograms cumulated over whole time period (17 or 20 days) covered by imaging data
CUM*N* parameters	prefix for quantities obtained from histograms cumulated over *N* days of data (one image per day)
AVG parameters	prefix for quantities representing the average of values obtained from histograms cumulated from single images (one day)
SD parameters	prefix for quantities representing the standard deviation of values obtained from histograms cumulated from single images (one day)
IM parameters	prefix for time-composite images—these images represent histogram quantities, such as MIN, MAX, AVG, MOD, taken from the time series of radiance values at each image pixel location
Region size 1	(60 × 60) pixels at full resolution (2·5° × 2·5°)
Region size 2	(60 × 120) pixels at full resolution (2·5° × 5°)
Region size 3	(90 × 180) pixels at full resolution (3·75° × 7·5°)
Region size 4	(120 × 240) pixels at full resolution (5° × 10°)

statistic calculated from the radiance times series at that location. We construct images of the VIS and IR MIN, MAX, AVG, and MOD. These images will be called IM-X (i.e. if X is MIN, the VIS MIN image will be called VIS IM-MIN). To separate the spatial and temporal contributions to the total variability, for each time composite image we calculate the differences between pairs of pixels in each as a function of their separation distance and the regional histogram statistics (mainly MOD) for comparison with the regional CUM parameters from the original images.

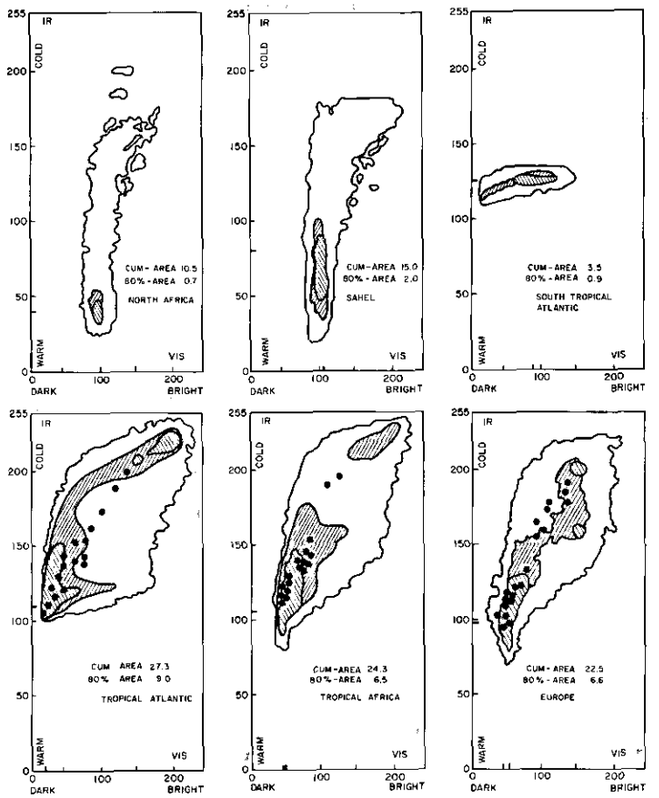

Figure 4. Bidimensional histograms of visible and infrared radiances measured by METEOSAT accumulated over 17 days in the smaller-sized special study regions shown in figure 1. Radiances are given as counts from zero to 255, representing visible intensity (abscissa) as a fraction of the solar constant in the instrument bandpass from 0 to 1 and IR brightness temperatures (ordinate) from 340 to 160 K, respectively. Contours indicate the frequency of occurrence of each pair of VIS–IR radiances, but the frequency values indicated by the contours are different for each distribution. The contours divide the total population: the outermost contour indicates the total population, the innermost contour contains 50 per cent of the population (indicated by left-slanting shading), and the intermediate contour contains 80 per cent of the population (indicated by right-slanting shading). The position of the node is indicated by small additional tick marks on the two radiance axes. The quantities CUM-AREA and 80 per cent AREA are defined in table 1. Each dot in the lower panels shows the average over the region of the visible/infrared radiances for a single day.

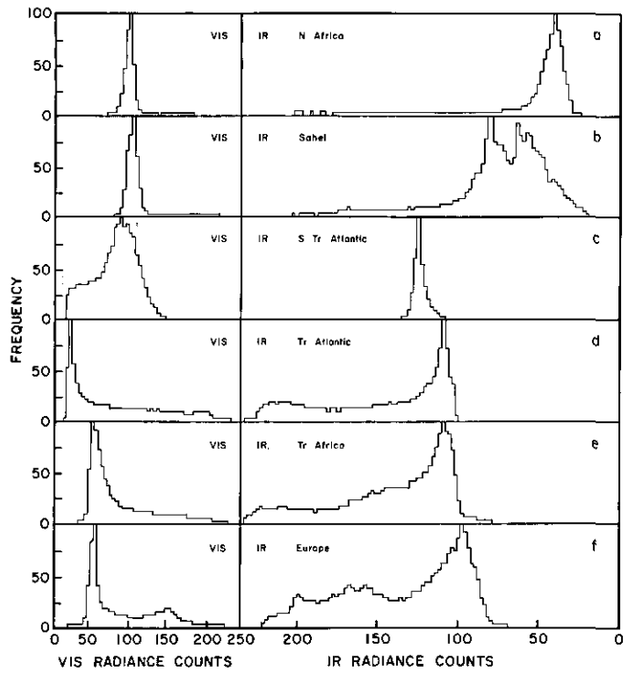

Figure 5. VIS and IR monodimensional radiance histograms from METEOSAT measurements accumulated over 17 days in the smaller-sized special study regions shown in figure 1 and associated with the bidimensional histograms in figure 4. Radiances are given in counts from zero to 255, representing visible intensity as a fraction of the solar constant in the instrument bandpass from 0 to 1 and IR brightness temperatures from 340 to 160 K. Frequency is shown is arbitrary units with the individual mode values set to 100 per cent.

4. Daily and time-cumulated histograms

4.1. *Regional distribution of histogram shapes*

The association of particular patterns in the radiance histograms with climate regimes is shown in figure 3, which displays the time-cumulated VIS–IR histograms for (60 × 120 pixels) subregions over the entire METEOSAT field of view for July 1983 and January 1984 (using data that have been spatially sampled to a 30 km spacing by taking one line out of six and one pixel out of six from the original images, see SR91). The well known climate regimes and their seasonal variations are apparent in the changes of histogram shapes with location and time. This figure motivates our examination of these shapes as a climate descriptor by suggesting that a few such shapes may be used to characterize the clouds and their seasonal variations in the major climate regimes.

4.2. *Regional histogram shape descriptions*

Seven regions, that represent all of the types of histograms seen in figure 3, are selected for detailed study (see figure 1). The bidimensional radiance distributions accumulated over 17 days in July 1983 for six of these seven regions are shown in figure 4. The associated monodimensional radiance distributions are displayed in figure 5. For two regions (Tr. Africa and Europe), sequences of daily histograms are shown in figure 6. The same characteristic histogram shapes described by Platt (1983) and Sèze and Desbois (1987) appear here.

The seven regions can be roughly gathered into three groups by their shapes in the radiance plane (figures 3, 4 and 5; table 2): Group 1 (N. Africa and Sahel), Group 2 (S. Atlantic), Group 3 (Tr. Africa, Tr. Atlantic, Europe and N. Atlantic).

4.2.1. *Desert regions (Group 1)*

The histogram shape characteristic of subtropical land has very small VIS radiance variation (small VIS SD), an elongated distribution along the IR axis (large IR SD), and a compact cluster of points at warm and (relatively) dark radiance values. The latter attribute is shown by a value of 80 per cent CUM-AREA that is much smaller than CUM-AREA. For N. Africa, the IR CUM-MAX reaches 55°C (table 2), VIS CUM-MIN is very bright (30–34 per cent), almost as bright as some clouds over the ocean (figure 5). The values of VIS CUM-MIN and IR CUM-MAX are also close to their respective MOD values and about 90 per cent of the VIS radiances are in the range CUM-MOD ± 4 per cent and 80 per cent of the IR radiances are in the range CUM-MOD ± 5 per cent. All of these features suggest low variability associated with the persistence of one condition over the area, in this case, clear conditions. The long low-frequency 'tail' in the IR histogram (figure 5) suggests the occasional presence of cold clouds that have a large influence on the CUM-SD: the coldest 5 per cent of the pixels explain 70 per cent of the IR variance. These clouds are relatively thin, however, since they have little effect on the VIS variance.†

For the Sahel, the 80 per cent CUM-AREA is more elongated along the IR axis due to a surface temperature gradient, associated with the presence of both desert and arid vegetation (Matthew 1983) in this area. More frequent occurrences of thin clouds and occasional thicker cirrus or altostratus also cause a sparse distribution of colder and brighter radiances (figure 4 and 5). Some of these clouds belong to the edges of squall lines passing to the south (cf. §§ 5 and 7, figures 12(*e*) and (*f*)). In spite of the variability of surface vegetation within the region, the VIS radiance distribution is no brighter than that in N. Africa with 95 per cent of VIS radiances in the range CUM-MOD ± 6 per cent. The larger VIS CUM-SD is due to the occasional appearance of some relatively bright clouds (70 per cent of the variance is explained by the brightest 3 per cent of the pixels).

Because of the approximate symmetry of the histogram shapes near the MOD, the average radiances (CUM-AVG) for these regions are close to the CUM-MOD and represent the regional surface properties well (table 2). The VIS PEAK being larger than the IR PEAK indicates that surface reflectances are less variable in time and space than surface temperatures (the precision of the VIS radiances is 2 per cent and the IR radiance precision is 0·75°C near 53°C). This characteristic is enhanced by the presence of the thin cold clouds, which increase the temperature variability with little effect on the scene reflectance (Platt 1983, Desbois and Sèze 1984a, Rossow *et al.* 1989b). The low VIS-IR COR and the low VIS–IR CUM-PEAK 2 (almost equal to the product of VIS CUM-PEAK 1 and IR CUM-PEAK 1) both indicate only a weak correlation between the variations of surface reflectance and temperature.

† Over brighter surfaces, it takes somewhat thicker cloud to change the VIS radiances by the same amounts, but optical depths are still < 10.

The cloud climatology obtained from surface observations (Hahn *et al.* 1984, Warren *et al.* 1985, 1986) for N. Africa shows (table 3) a very high frequency of clear sky, somewhat lower for the Sahel. The most frequent and extensive clouds are cirrus (average amount about 5–10 per cent over N. Africa and 15–25 per cent over the Sahel) and altostratus (5–10 per cent over N. Africa and 20 per cent over the Sahel). However, this climatology also reports the occurrence of some low clouds (cumulus and stratus amounts of about 5 per cent). These low-level clouds are less prevalent in our 12 UT images because of their diurnal variation (peak magnitude, <30 per cent, occurs in mid-afternoon), although the occurrence of some of these clouds may explain, in part, the somewhat larger 80 per cent CUM-AREA in the Sahel.

4.2.2. *Sub-tropical ocean regions (Group 2)*

These histograms have a very small IR radiance variation, but a significant VIS radiance variation (figure 4), which is characteristic of low-lying stratocumulus cloud layers over subtropical oceans (figure 3; Hartmann and Short 1980, Cahalan *et al.* 1982). The S. Atlantic is one of only a few regions in the METEOSAT view that is so dominated by large amounts of very persistent cloudiness (Saunders 1985, Coulmann *et al.* 1986) that the high-frequency part of the histogram represents

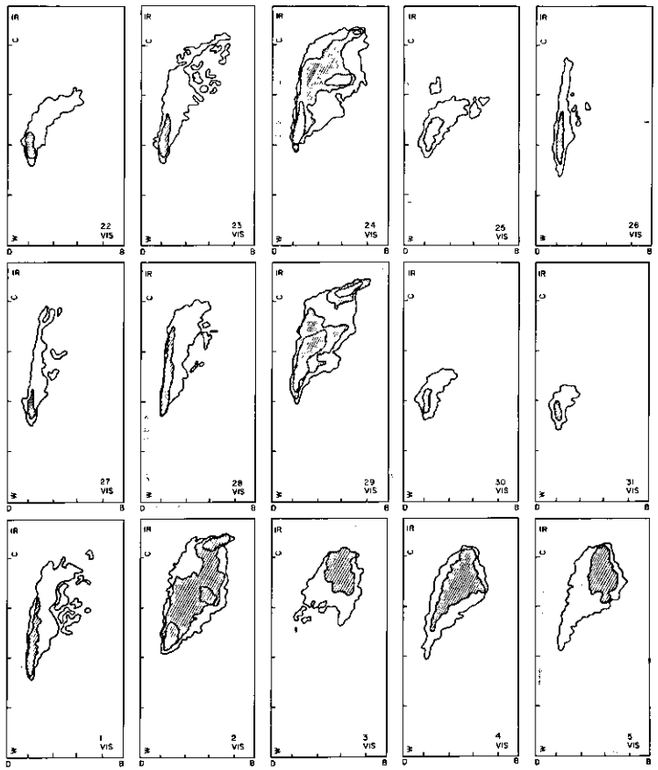

(*a*)

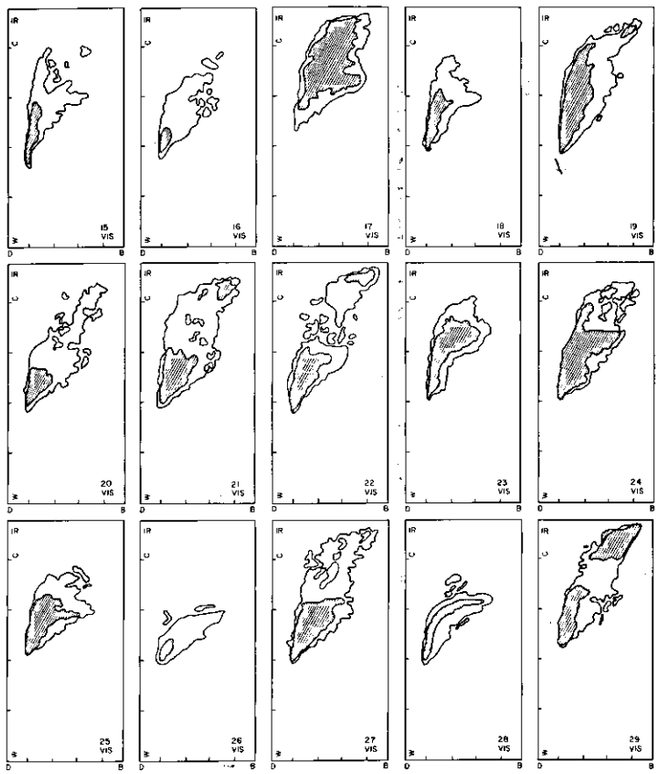

(*b*)

Figure 6. Daily bidimensional radiance histograms for (*a*) Europe and (*b*) Tr. Africa for two weeks, illustrating the variation of histogram shapes in comparison with the time-cumulated shapes shown in figure 4. Radiance axes are the same as in figure 3. The contours indicated the same frequencies as defined for the cumulated distributions, which differ between Europe and Tr. Africa. Shading indicates the 80 per cent portion of the total population. Days in July and August are indicated by the numbers in the lower right-hand corner of each histogram.

cloud properties, rather than surface properties. Nevertheless VIS MODI is less than that in N. Africa (table 2). VIS CUM-MIN and IR CUM-MAX are much further away from their respective MOD values than in other regions and are not always characteristic of the surface (see §§ 5 and 7), even though the cloud cover is close to its minimum at this time of the day (Minnis and Harrison 1984, Duvel and Kandel 1985, Hartmann and Recker 1986). The VIS radiance distribution (figure 5) has a broad peak at larger values than typical of most other oceanic regions. This peak is nearly in the centre of the VIS range CUM-MOD $\pm$ 14 per cent; however the frequencies decrease more slowly on the low side of VIS-MOD and more sharply on the high side. In contrast to the other regions, VIS CUM-AVG is smaller than VIS-CUM-MOD. Since the pixels with larger VIS radiances are probably completely covered by cloud, pixels on the low side of the MOD are either partially covered (Coakley and Bretherton 1982) or optically thinner or both (Coakley *et al.* 1987).

Table 2. VIS and IR CUM (first line), AVG (second line) and SD parameter (third line) values, given in count values, for the seven regions (60 × 120 pixels). One count is approximately equivalent to 0·5 per cent for VIS and 0·5°C for IR. For IR the lowest values correspond to MAX temperatures and the highest values to MIN temperatures.

					VIS					
REG	MIN	MAX	AVG	MOD1	PEAK1	MOD2	PEAK2	SD	COR	SURF
	64	172	90	92	31	92	5	6	0·1	11
N. Afr.	70	120	90	91	33	91	8	6	−0·2	2
	2	18	1	2	4	3	3	1	0·4	2
	72	204	95	96	26	96	2	11	0·4	15
Sah.	75	146	95	97	29	96	5	8	0·3	4
	2	28	5	3	6	4	2	6	0·3	0·2
	12	136	72	80	7	76	3	27	0·7	3
S. Atl.	17	124	71	68	10	73	6	22	0·6	2
	9	8	14	30	3	27	3	5	0·2	0·5
	8	220	64	16	15	16	3	53	0·9	27
Tr. Atl.	13	193	64	37	17	46	7	41	0·8	13
	2	33	31	55	13	67	7	14	0·1	5
	28	216	74	44	13	44	2	38	0·9	24
Tr. Afr.	33	191	74	57	15	60	3	29	0·8	11
	4	22	22	31	7	42	3	10	0·1	4
	16	212	79	48	17	44	1	40	0·9	23
Eur.	30	169	79	72	20	80	3	21	0·6	9
	10	32	32	40	12	47	2	10	0·3	4
	12	156	62	16	12	16	4	32	0·5	15
N. Atl.	15	129	62	45	15	40	6	27	0·4	8
	3	14	16	37	13	33	9	5	0·2	2
	MAX	MIN			IR					
	23	201	42	38	14	38	5	11	0·1	11
N. Afr.	28	91	42	38	19	37	8	8	−0·2	2
	4	49	6	5	6	4	3	6	0·4	2
	18	203	71	78	5	78	2	26	0·4	15
Sah.	35	153	71	66	10	66	5	19	0·3	4
	14	32	17	14	4	15	2	6	0·3	2
	109	134	124	124	32	124	3	3	0·7	3
S. Atl.	113	129	123	124	46	123	6	3	0·6	2
	4	2	2	2	19	4	3	1	0·2	0·5
	100	232	144	108	8	108	3	38	0·9	27
Tr. Atl.	105	214	144	127	13	127	7	28	0·8	13
	5	28	24	39	11	43	7	10	0·1	5
	79	233	136	108	5	104	2	33	0·9	24
Tr. Afr.	95	212	136	124	8	121	3	24	0·8	11
	8	15	22	35	4	38	3	8	0·1	4
	69	221	132	96	4	96	1	36	0·9	23
Eur.	92	192	132	132	9	130	3	19	0·6	9
	15	29	30	44	3	46	2	8	0·3	4
	116	214	140	128	8	120	4	18	0·5	15
N. Am.	119	195	140	131	15	126	6	15	0·4	8
	2	15	9	11	11	5	9	5	0·2	2

The pixels on the high side may either be optically thicker than normal or may be related to variations of reflectance with viewing geometry (Welch *et al.* 1988).

As a consequence of the strong layering of these low-level clouds with top temperatures very near the surface temperature, the IR CUM-SD is very small (CUM-AREA is very small) and the IR CUM-AVG is equal to the IR CUM-MOD (table 2). Unlike all the other regions, the IR PEAK1 is larger than the VIS PEAK 1, indicating less variation of the cloud temperatures than of their reflectances. For more cloudy regions the VIS-IR CUM-COR is much higher, but the layering of the clouds in the S. Atlantic near the surface reduces VIS-IR CUM-COR to about 0·7.

The high coverage and persistence of these stratocumulus layers is shown in the Warren *et al.* climatology (table 3). Although our observations (1230 local time) are close to the minimum of the cloud diurnal cycle, the 20–25 per cent amplitude of this cycle (Kandel and Duvel 1985, Saunders 1985, Coulmann *et al.* 1986, Minnis and Harrison 1984) is not sufficient to eliminate the nearly total coverage by these clouds (see §7). This suggests that some satellite estimates may be mistaking optical thickness variation for cloud-cover variation. Warren *et al.* (1988) report small amounts of altostratus (about 20 per cent) and cirrus (about 5 per cent) in this region, mostly near the coast of Africa. We see very little evidence for such colder clouds in July 1983, but they are more prevalent near Africa in January 1984 (figure 3).

4.2.3. *Tropical and middle latitude regions (Group 3)*

These histograms have large dispersions (large values of CUM-AREA, 80 per cent CUM-AREA and SD) in both the VIS and IR radiances (figure 3, 4 and 5; table 2) which is characteristic of a mixture of different kinds of clouds at different levels: multi-layer convective complexes and low clouds over the sea (Tr. Atlantic), a mixture of high-, middle- and low-level clouds in a convective regime over land (Tr. Africa), and high, middle and low cloud layers over land (Europe) and ocean (N. Atlantic) (Warren *et al.* 1986, 1988). The predominance of clouds is indicated by VIS AVG > VIS CUM-MOD and IR AVG < IR CUM-MOD. The histograms of this group have the brightest and coldest clouds (table 2: for the ITCZ,

Table 3. Cloud climatology for seven study regions based on surface weather observations (Hahn *et al.* 1982, 1984, Warren *et al.* 1985, 1986). Seasonal mean quantities shown are total cloud amount in per cent (CA), percentage frequency of occurrence (f_0), and probability of a cloud type occurring alone (p_s). Cloud types are stratus (St), cumulus (Cu), altostratus (As), nimbostratus (Ns), cirrus (Ci), and cumulonimbus (Cb).

		St		Cu		As		Ns		Ci		Cb	
Region	CA	f_0	p_s	f_0	p_s	f_0	p_s	f_0	p_s	f_0	p_s	f_0	p_s
N. Africa	20	5	29	15	41	24	31	—	—	22	37	3	20
Sahel	40	7	9	39	44	42	1	—	—	49	43	12	12
S. Atl.	77	72	57	18	68	33	9	1	—	13	16	4	46
Tr. Atl.	75	42	29	31	44	65	7	7	11	53	9	20	21
Tr. Africa	73	19	6	20	24	66	18	2	—	62	16	28	11
Europe	58	42	20	20	38	42	20	8	—	42	22	28	11
N. Atl.	80	70	27	18	36	51	8	11	8	45	12	7	24

IR-MIN = −77°C and VIS-MAX = 100 per cent; for Europe, IR-MIN = −58°C and VIS-MAX = 100 per cent) and the largest CUM-SD and AVG-SD both in VIS and IR. About 50 to 60 per cent of the variance is explained by the coldest and brightest 20 per cent of the pixels. Even the day-to-day variability of the daily average radiances (SD-AVG) is large (Cahalan *et al.* 1982, Hartmann and Recker 1986), although it is smaller than the average of the daily values (AVG-SD) and the CUM-SD due to the significant variability inside individual clouds. The large dispersion is also shown by the predominance of low frequencies in the histograms (figure 2 and 4).

The VIS/IR COR is high (0·8–0·9 for the ITCZ and Europe), which is characteristic of regions with high and/or middle cloud cover with variable optical thickness (reflectivity/emissivity) and/or partial coverage of the pixels (Hartmann and Short 1980). However, the high correlation does not require a linear relation between the VIS and IR radiance variations (see below); instead the high-frequency parts of the histograms (figure 4 and 6) show a variety of radiance patterns. The North Atlantic histogram (not shown) is similar in shape to the other histograms in this group, but more compact due to colder sea surface temperatures and the more limited range of VIS radiances occuring at larger solar zenith angles at higher latitudes. These decreases in the range of variation of the VIS and IR radiances are not correlated and reduce the CUM-COR (table 2).

Generally, the VIS and IR MOD radiances correspond to surface properties (clear conditions) (figure 4 and 5), even with large cloud-cover amounts, because of the much lower variability of the surface compared with the clouds, especially over the ocean. This conclusion is supported by the small separations of VIS CUM-MIN from VIS CUM-MOD and IR CUM-MAX from IR CUM-MOD (similar to clear deserts and the clear western portions of subtropical oceans). A large part of the 50 per cent CUM-AREA is situated in the relatively warm and dark part of the histogram, 40 to 50 per cent of the pixels have a reflectance in the range CUM-MOD ± 4 per cent, and 35 to 40 per cent have a brightness temperature in the range CUM-MOD ± 5°C. The limited range of variation is also an indication that there are frequent occurrences of very thin clouds or small, broken low- or middle-level clouds that do not alter the radiances very much (Sèze and Desbois 1987). For the N. Atlantic where the amounts of cloud is large, only 20 per cent of the pixels have a reflectance in the range CUM-MOD ± 4 per cent; but 60 per cent of the pixels have a brightness temperature in the range CUM-MOD ± 5°C (i.e. the persistent low cloud layer present in this region has a temperature very close to the sea surface temperature).

A secondary peak can appear in the histograms at larger VIS radiance values because the rate of increase of cloud reflectance with increasing liquid water content decreases as the reflectance approaches an asymptotic value for very large optical thicknesses. Secondary peaks are also present at colder values in the IR distributions (e.g. figure 5 for Tr. Africa and Europe) more often than for the VIS histograms, due to the occurrence of cloud layers and a dynamic limit on the height of clouds associated with the tropopause. Although the diurnal minimum of deep convection over Tr. Africa occurs at about noon (Duvel and Kandel 1985, Del Genio and Yao 1987, Desbois *et al.* 1988, Duvel 1988), a secondary frequency peak still appears in the coldest and brightest part of the bidimensional histograms (figure 4).

The multi-layer nature of the cloud cover for these regions is obvious in the ground-based climatology (table 3; see Hahn *et al.* (1982, 1984), Warren *et al.* (1985, 1986, 1988)). All of these regions are characterized by the frequent occurrence of cirrus, altostratus and low-level clouds. Tr. Africa has the largest occurrence of cirrus and altostratus (above 60 per cent), but the lowest occurrence of low clouds (40 per cent); however, at the minimum in the dirunal cycle the percentage of cirrus and altostratus may be lower (Del Genio and Yao 1987, Duvel 1988). Cumulonimbus are present in the tropical regions, but their areal coverage is small compared to the other cloud types: the frequency peak that we find in the time cumulated histograms is caused more by the small variability of the brightest and coldest parts of these clouds than by their frequency of occurrence. We note that for N. Atlantic the percentage of stratus is as high as in S. Atlantic.

Despite the overall resemblance of time-cumulated histogram shapes (figure 3 and 4), the nature of the time variations differs between the tropical and midlatitude regions (see § 5). In the daily histograms (figure 6), the extent of the hatched areas delineating the 80 per cent isolines is highly variable from day to day. In contrast, the time-cumulated histograms are characterized by a relatively small 80 per cent CUM-AREA in spite of their larger overall size (CUM-AREA). This behaviour is magnified for 50 per cent CUM-AREA. The tropical regions can be characterized as having a similar large spatial variability of cloud properties every day, while the midlatitude region exhibits less spatial variability on many days with more variation of histogram shape from one day to another (Figures 6 and 8).

Figure 4 also shows the daily average radiances for several regions. These values have often been used to describe the mean properties of cloud fields in a region (Hartmann and Short 1980, Cahalan *et al.* 1982, Hartmann and Fecker 1986, Duvel 1988), but, as can be seen, these average values do not always lie in the high-frequency part of the histograms, because of the nonlinear relationship between the VIS and IR cloudy radiances, especially in multi-layer cloud systems. In some

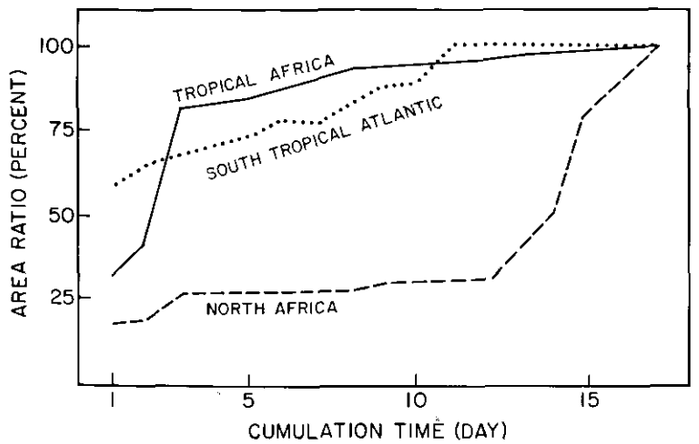

Figure 7. Evolution of the surface area covered by the bidimensional distribution of radiances (CUMN-AREA—see table 1) as a function of the cumulation time period for N. Africa, S. Atlantic and Tr. Africa. The histogram area indicates the number of distinct radiance values that have occurred out of the total number of possibilities; these areas are expressed as the fraction of the total area in each region after 17 days (CUM-AREA), indicated in figure 4.

regions with very low frequency of clear conditions (figure 4), the spatially averaged radiances, even in a time series, cannot be used to describe the radiance variations.

5. Temporal evolution of histogram shapes

5.1. *Time-cumulated histogram evolution*

The time evolution of the radiance distributions, as shown by the changes in the CUM*N* parameters as *N* increases, shows that MIN, MAX, MOD1, and MOD2, and AVG exhibit a rapid variation between 1 and 5 days and then a much weaker variation after that. The PEAK2 generally decreases with time and becomes stable only after about 10 days. The other parameters are more variable, though their variability (SD) is small compared to their day-to-day variations (AVG-SD).

The fraction of 17 day total histogram surface area (CUM-AREA) occupied by the VIS–IR distributions cumulated over variable time periods (CUMM-AREA) is displayed in figure 7 for representatives of each group. Generally, after 5 to 10 days, the area occupied by the cumulated histograms in the VIS–IR radiance space is nearly constant, having almost reached the full value. However, in some cases this percentage can suddenly increase on a specific day when some rare event happens, such as cirrus over N. Africa or cirrus over the S. Atlantic.

Rapid increase in 80 per cent AREA and decrease of PEAK2 over 5–10 days intervals and their much weaker variation over longer intervals is caused by a trend toward a more homogeneous distribution of frequencies inside the 80 per cent AREA as the cumulation period increases. In Europe, however, 80 per cent AREA

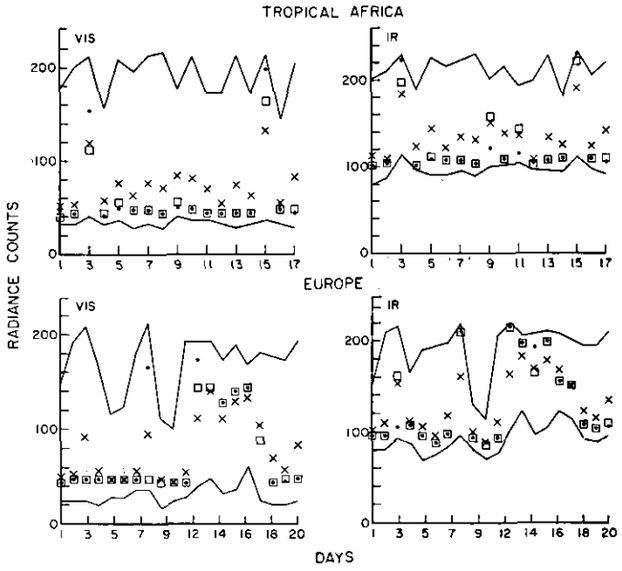

Figure 8. Time variation of radiance distribution statistics from daily histograms for Tr. Africa (upper) and Europe (lower). The left-hand panel for both regions shows the MAX and MIN (solid lines) and the AVG (X), MOD1 (square), and MOD2 (dot) for VIS (see table 1); the same quantities for IR are shown in the right-hand panels. Low IR counts correspond to warm temperatures.

continues to increase up to 17 days, because of the longer time scale for synoptic variations of the cloud cover (c.f. figures 6 and 7).

5.2. *Daily and time-cumulated histograms*

The comparison of the CUM and AVG parameters and the magnitude of the SD parameters (see tables 2 and 5, figures 7 and 8) reveals differences that indicate the relative contribution of day-to-day radiance variability to the total cumulated variability (see also figure 6). For the desert regions, the small ratio of AVG-AREA to CUM-AREA is associated with a high frequency of clear conditions, which exhibit little variability. For the S. Atlantic, the ratio is larger (50 per cent), associated with persistent (time-stable), widespread cloud cover with little spatial variability (small AVG-AREA); however, AVG-SD < CUM-SD and some variability in the CUM*N* parameters are related to a larger temporal than spatial variability of the visible radiances (Coakley and Bretherton 1982). A similar ratio between the AVG-AREA and CUM-AREA occurs in the N. Atlantic region, but in that case it is associated with the temporal stability of cloud cover with relatively large spatial variability (large AVG-AREA, small difference between the AVG-SD and CUM-SD).

Table 4. Statistics of VIS and IR radiance differences. COR1 is correlation between radiances separated by one day. AVG1 and AVG3 are the average differences for time separations of 1 and 3 days; r.m.s.1 and r.m.s.3 are the corresponding root-mean-square differences. Also given are the r.m.s. differences between any possible pair of pixels during the period (CUM-r.m.s.) and the root-mean-square differences of the daily radiance averages (r.m.s.-AVG).

REG	COR1	AVG1	r.m.s.1	AVG3	r.m.s.3	CUM-r.m.s	r.m.s.-AVG
N. Africa							
VIS	0·76	2	4	2	4	9	1
IR	0·32	7	13	9	13	16	9
Sahel							
VIS	0·28	6	13	7	15	16	7
IR	0·28	22	31	30	39	37	24
S. Atlantic							
VIS	0·30	25	32	30	37	38	20
IR	0·24	3	4	4	5	5	3
Tr. Atlantic							
VIS	0·01	57	74	62	78	75	44
IR	−0·01	42	53	44	54	54	34
Tr. Africa							
VIS	−0·09	41	53	38	53	53	31
IR	−0·16	40	49	38	48	47	31
Europe							
VIS	0·43	29	43	38	52	56	45
IR	0·39	30	41	42	52	51	42
N. Atlantic							
VIS	0·15	33	41	35	44	45	23
IR	0·07	18	25	19	25	28	13

Table 5. VIS and IR CUM (first line), AVG (second line) and SD parameter (third line) values for the seven regions (120 × 240 pixels). See legend in table 2 for definitions. IR MIN/MAX refers to warmest/coldest temperatures.

				VIS						
REG	MIN	MAX	AVG	MOD1	PEAK1	MOD2	PEAK2	SD	COR	SURF
	12	192	80	88	15	92	2	17	−0·5	27
N. Afr.	15	134	80	89	17	89	3	17	−0·6	8
	2	26	1	3	1	3	1	1	0·3	4
	48	212	89	88	17	92	1	13	0·4	26
Sah.	52	175	89	88	18	93	2	12	0·4	11
	2	23	3	3	2	6	0	4	0·2	3
	8	144	73	88	6	88	2	29	0·7	6
S. Atl.	9	136	73	68	7	73	4	27	0·7	3
	2	7	10	31	2	29	1	4	0·2	1
	8	244	65	16	13	16	3	51	0·8	31
Tr. Atl.	11	213	65	20	14	26	5	46	0·8	21
	1	18	20	13	10	41	5	11	0·1	5
	24	224	74	44	12	44	2	37	0·9	28
Tr. Afr.	27	209	74	46	13	53	2	34	0·8	19
	3	11	14	2	5	36	1	7	0·	3
	12	212	73	48	20	48	2	36	0·8	28
Eur.	16	186	73	59	21	54	2	28	0·7	15
	4	18	20	28	11	31	1	9	0·1	4
	12	168	63	16	9	16	3	32	0·5	19
N. Atl.	13	148	63	41	11	34	3	29	0·5	12
	2	12	12	35	6	31	3	3	0·1	1
	MAX	MIN			IR					
	6	206	48	38	10	38	2	19	−0·5	27
N. Afr.	22	136	48	40	12	39	3	17	−0·6	8
	5	36	6	3	4	4	1	6	0·3	4
	0	209	70	62	4	62	1	30	0·4	26
Sah.	16	175	70	66	6	66	2	26	0·4	11
	13	21	14	15	2	13	0	6	0·2	3
	107	178	124	124	31	124	2	3	0·7	6
S. Atl.	109	135	123	125	40	123	4	3	0·7	3
	1	13	1	2	12	5	1	1	0·2	1
	98	232	142	108	8	108	3	37	0·9	31
Tr. Atl.	101	223	142	115	10	113	5	31	0·8	21
	3	13	17	26	8	27	5	9	0·1	5
	78	235	137	108	5	104	2	34	0·8	28
Tr. Afr.	88	226	137	120	6	112	2	30	0·8	19
	5	7	15	33	2	29	1	5	0	3
	62	221	126	96	4	96	2	33	0·8	28
Eur.	76	212	126	118	6	106	2	26	0·7	15
	7	5	19	32	2	25	1	6	0·1	4
	113	217	141	130	7	120	3	19	0·5	19
N. Atl.	117	207	141	130	11	125	3	18	0·5	12
	2	7	6	8	4	6	3	3	0·1	1

For the two ITCZ areas and Europe, the multi-layer cloud cover leads to higher average histogram areas (larger spatial variability), but also to a higher standard deviation around the average (larger time variability). A distinction can be made between regions where multi-layer systems are common every day (Tr. Africa) and regions where large changes in cloud cover characteristics occur during the period (Europe) (see figure 6). In Tr. Africa the daily histograms usually have large AVG-AREA; in Europe the daily histograms have lower AVG-AREA but are more variable from day to day (larger SD-SURF). For Tr. Atlantic, the variability of some parameters and the variability of the daily histogram shapes are related to the presence of a persistent (background) of low-level clouds with day-to-day variations of the higher level cloudiness associated with moving squall lines (table 2).

5.3. *Variation of radiances with time scale*

For each pair of images separated by N days, the absolute difference in radiances at each location is computed. Then for each N day separation (for N between 1 and 5) the distribution of these differences is collected and the average and r.m.s. values computed. The correlation between image pairs separated by N days is also computed. The average and r.m.s. differences for 1 and 3 day separations, together with the correlation for a one day separation,† are reported in table 4. Also shown in Table 4 are the r.m.s. radiance differences between any possible pixel pair during the period (CUM-r.m.s.) and the r.m.s. differences between all the possible pairs of daily average radiances (r.m.s.-AVG).

For a one day separation, the r.m.s. difference is already close to CUM-r.m.s. (Cahalan *et al.* 1982); exceptions are the desert regions, especially in VIS, and Europe, due to the lower temporal than spatial variability of the surface properties. Between 1 and 3 days a slight increase in variability appears in the visible for the cloudy regions. For 3 days separation, the r.m.s. differences are of the same order as the CUM-r.m.s. (e.g. the correlation is close to zero). For separations larger than 3 days, the differences seem to vary randomly about the difference value found for the 3 day separation, except for Europe where differences continue to increase up to a 5 day separation. Europe is also the region for which the increase in average differences between 1 and 3 days is the highest, consistent with the larger synoptic time scale for significant changes of weather conditions. This is also illustrated by large changes in histogram shapes indicating major evolution in the cloud cover during the period (figure 6 and 8): the first part is characterized by clear sky and cirrus, while the second part by more multi-layer systems with a high frequency of middle-level clouds. For Tr Africa, the temporal variability seems independent of the time scale, which is in agreement with the relative constancy of the daily histogram shapes and statistics, indicating the predominance of a shorter timescale.

The low correlation and high variability found between radiance images for the 1–5 day scales can be caused by the absence of any characteristic time scale in this range or by the large spaitial variability of cloudiness moving through fixed

† The correlation between radiance images, separated by N days, can be estimated from the values of N day r.m.s. and CUM-SD by

$$1-\tfrac{1}{2}(N \text{ day r.m.s.}/\text{CUM-SD})^2$$

if we assume that the mean and variance of the time distribution are not time-dependent (Matherton 1977). This relation implies that, as the r.m.s. value approaches CUM-r.m.s., the correlation goes to zero.

locations. A previous study by Cahalan *et al.* (1982), using spatially averaged IR radiances on a 2·5° × 2·5° grid, exhibited larger autocorrelations for a 1 day lag than the autocorrelations we have found for single pixels, but they show how the advection of clouds can produce this effect. They found only a very small increase in the correlations at larger averaging scales. Duvel (1988) examined the dominant time scale of radiance fluctuations in METEOSAT data by using the percentage of the total variance explained by the different time scales. He found more variance explained by changes in 2·6 to 8·4 day periods for Sahel, Tr. Atlantic and Tr. Africa and roughly equal contributions from the 2·6 to 8·4 and >9·2 day periods for N. Africa, N. Atlantic and Europe. The S. Atlantic is the one region where more variation occurs on periods >9·2 days. Therefore, although our analysis does not cover a long enough period of time to determine the predominant time scales, our results give the same qualitative relations between tropical and midlatitude time scales as found by Cahalan *et al.* (1982) and Duvel (1988). On the other hand, these results suggest that spatially averaged data (used by both Cahalan *et al.* and Duvel) underestimate the overall radiance variability as shown by the comparison of the r.m.s.-AVG and the CUM-r.m.s. (table 4).

6. Spatial stability of histogram shapes

The stability of the radiance distribution shapes cumulated over various spatial scales is tested by varying the size of the studied region from (60 × 60) pixels to (120 × 240) pixels (equivalent to latitude–longitudes ranging from 2·5° × 2·5° to 5° × 10° at the subsatellite point). The statistics of (60 × 120) regions are given in table 2 and are to be compared with the values of (120 × 240) regions given in table 5.

The spatial variability of the radiances on scales smaller than the smallest region is indicated by the absolute difference in radiance between pairs of pixels separated by N pixels, where N varies from 1 to 70 pixels in the east–west direction (5 to 350 km at low latitudes and 10 to 700 km at high latitudes) and from 1 to 45 pixels in the north–south direction over 17 (or 20) days. For each region and each N, the average, standard deviation, mode, minimum, maximum and r.m.s. values of the absolute *difference* distributions have been computed.

6.1. *Evolution of the CUM and AVG parameters with region size*

CUM parameters for a given area change little with increasing region size. Exceptions are CUM-AREA, which tends to increase with the region size, and CUM-PEAK (especially VIS-IR CUM-PEAK) which decreases. In figure 9, we see a slight increase (about 6 per cent) in the CUM-AREA with increasing size of most regions, but the histogram shape does not change very much (figure 10). In certain cases, there are larger increases in CUM-AREA and an evolution in shape because of changes in the surface properties included in the region (especially at land/ocean boundaries in Europe and N Africa), latitudinal changes in surface temperature (Europe, Sahel), solar zenith angle variations (N Atlantic), or changes in the cloud regime (appearance of altostratus in S Atlantic, increasing cloudiness in the southern part of Sahel). However, these variations in total histogram shape are often produced by a very small percentage of the pixels; significant changes in the radiative properties of a region are revealed by changes in the 80 per cent and 50 per cent CUM-AREA.

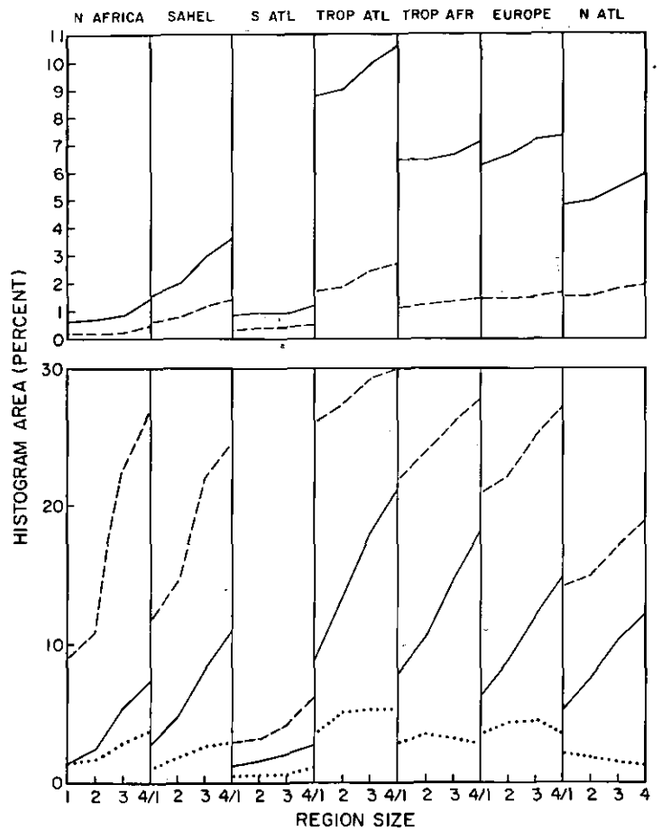

Figure 9. Evolution of various measures of the time-cumulated radiance histogram shapes with increasing region size for the seven special study areas. The upper panels show the values of 80 per cent-CUM-AREA (solid) and 50 per cent-CUM-AREA (dashed). The lower panels show total CUM-AREA (dashed), AVG-AREA (solid), and SD-AREA (dotted). Values for the four region sizes are shown in increasing order from left to right in each panel: 1 = 60 × 60 pixels, 2 = 60 × 120 pixels, 3 = 90 × 180 pixels, and 4 = 120 × 240 pixels.

Some significant differences occur between the radiance variability on a specific day and over the whole period when region size is increased. The AVG-SD increase with region size is significant, while the CUM-SD stays relatively stable; hence the AVG-SD for region size 4 is often closer to the CUM-SD value. This occurs when the region size becomes large enough that both clear sky and high cloud are more likely to be found within the region. The same conclusion is reached by looking at the increases in IR AVG-MIN (colder cloud) and VIS AVG-MAX (brighter cloud) and at the decreases of the IR AVG-MAX (warmer surface) and VIS AVG-MIN (darker surface). The VIS and IR AVG-MOD1 also tend to converge (i.e. decrease and increase, respectively) to the clear sky values as the region size increases. The corresponding CUM-parameters are relatively constant, especially in cloudy

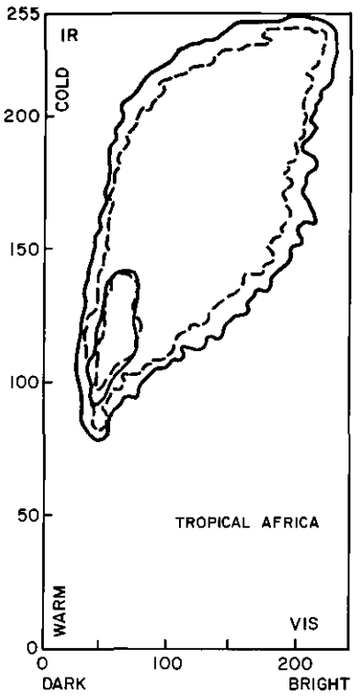

Figure 10. Radiance histograms for Tr. Africa illustrating the effect of cumulation over a smaller (dashed) and larger (solid) geographic region. Results are shown for 60×60 pixels and 120×240 pixels. The outermost contours in the bidimensional histogram contain 100 per cent of the population, while the innermost contours contain 50 per cent.

regions. This difference in evolution between the CUM parameters and AVG parameters leads to a convergence of the two sets of parameters as the region size increases (tables 2 and 5); and, except for the SD-SURF in certain cases, most of the SD parametrers also decrease with region size (for the SD-AVG, see Short and Cahalan (1983)).

6.2. *Effect of region size on histogram time-evolution*

For the ITCZ and N Atlantic regions, 88 per cent of the possible radiance values occur after 3 to 5 days for 120×240 pixel regions, but for 60×60 regions, it takes 7 to 9 days to reach the same percentage. There are also larger differences in AREA between different region sizes for cumulations over shorter time periods, but a relative constancy of the differences for cumulation time periods longer than 5–10 days. This suggests that some of the region-size-dependent differences are systematic, usually due to variations in surface properties. For the S. Atlantic and desert regions, the behaviour is very dependent on which days are included in the statistics (figure 7); the occurrence of rare events during the period lengthens the time for convergence of the statistics. Increasing the region size increases the probability of occurrence of these rare events. In the desert regions, the higher probability for the

occurrence of thicker cirrus in the larger region produces a strong decrease of IR CUM-MIN. In the S. Atlantic, the more likely appearance of cirrus in the larger region decouples VIS CUM-MAX and IR CUM-MIN; they can correspond to two different clouds occurring at different times.

6.3. *Variation of radiances with spatial scale*

For a given separation distance, the distributions of absolute radiance differences between pixels are asymmetric with a mode at very small values. The average difference increases with separation distance (table 6, figure 11) and the mode difference frequency decreases. The largest increase in average difference with distance is found for separations of 1 to 5 pixels (5 to 25 km at nadir). As the distances become larger, the rate of increase decreases. The maximum difference

Table 6. Statistics of VIS and IR radiance differences for spatial separations of 1, 5, 19 and 70 pixels over a 17 or 20 day period for the seven regions. The statistics are the maximum VIS difference, average of the absolute VIS difference, average IR difference, and maximum IR difference (first column) and the square root of the mean square VIS and IR differences (second column). Also given are the root mean square differences of the daily radiance averages (r.m.s.–AVG) and the r.m.s. differences between any possible pair of pixels during the period (CUM-r.m.s.).

	MAX1		MAX5		MAX19		MAX70		r.m.s.-	CUM-
REG	AVG1	r.m.s.1	AVG5	r.m.s.5	AVG19	r.m.s.19	AVG70	r.m.s.70	AVG	r.m.s.
N. Africa	36		44		48		48			
VIS	1	3	3	5	4	6	8	12	8	9
IR	1	3	2	8	5	12	7	17	14	16
	129		157		158		160			
Sahel	72		108		108		116			
VIS	1	3	3	7	5	9	10	14	0·4	14
IR	2	4	6	12	10	18	19	26	28	37
	50		117		132		141			
S. Atlantic	76		104		104		108			
VIS	8	11	12	17	18	24	26	33	32	38
IR	1	1	1	2	2	3	3	4	4	5
	9		16		19		19			
Tr. Atlantic	96		164		196		196			
VIS	8	13	19	29	31	45	47	65	62	76
IR	3	5	10	16	19	28	33	46	42	54
	43		99		115		122			
Tr. Africa	100		168		180		172			
VIS	9	14	18	28	26	39	33	47	43	53
IR	4	6	13	18	21	28	29	39	35	47
	53		120		135		128			
Europe	88		136		144		164			
VIS	6	10	12	19	17	27	23	36	33	56
IR	3	5	8	13	14	21	23	33	29	51
	50		98		112		125			
N. Atlantic	72		112		116		136			
VIS	6	9	14	20	24	32	33	42	38	45
IR	2	4	6	10	10	16	18	24	22	28
	35		73		83		84			

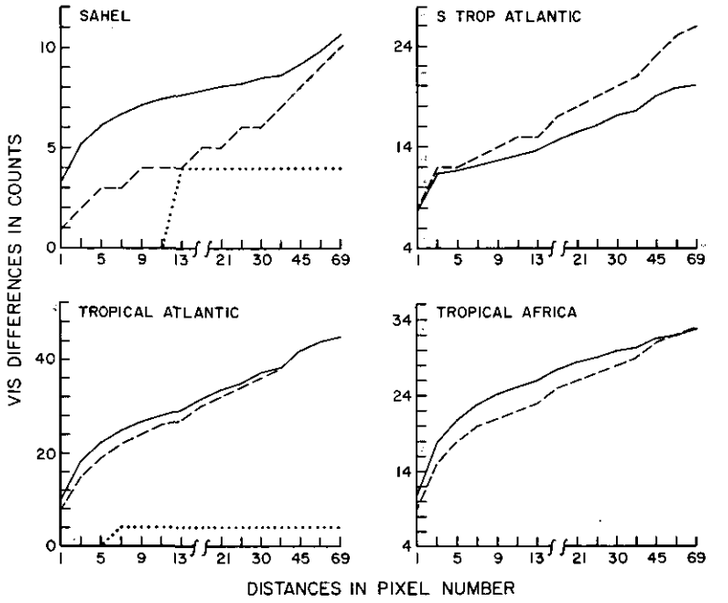

Figure 11. Evolution of the average (solid), mode (dashed) and standard deviation (dotted) of (*a*) VIS and (*b*) IR radiance differences as a function of the separation distance (in pixels) for the Sahel, S. Atlantic, Tr. Atlantic and Tr. Africa. A missing dotted line indicates that the standard deviation of the differences is very near zero.

also increases dramatically from 1 to 5 pixels and then becomes almost independent of separation distance. In spite of the high surface variability of the desert regions, the smallest differences are found for N. Africa and Sahel; an exception to generally higher radiance differences in cloudy regions is the stratocumulus layer in S. Atlantic in IR. In agreement with the discussion of time variations, larger radiance differences are found for the daily histograms in the ITCZ regions than for Europe.

Except for the 1 to 5 pixel length scales, where a strong increase in the radiance spatial heterogeneity appears, no characteristic jump in these differences suggests a privileged larger scale between 5 and 70 pixels. However, the latitudinal differences often are larger than the longitudinal differences for the same length scale (Cahalan *et al.* 1982). That the AVG-SD increases somewhat with region size indicates that the spatial radiance differences do continue to increase for larger spatial scales; however, this increase does not appear to be very rapid.

The radiance differences (correlations) for a spatial separation of 70 pixels are smaller (larger) than the 3 day radiance differences or, at the most, equal (compare tables 4 and 6), which agrees with the CUM-SD being larger than the AVG-SD. Exceptions are the desert regions in VIS: for N. Africa, the temporal stability of the VIS radiances is very high, higher than the spatial stability of radiances at separations greater than 5 pixels.

7. Relation between time-cumulated and time-composite image statistics

Time-composite images (figure 12) show the spatial patterns of some statistics (average, mode, minimum, maximum) obtained from the radiance variations with time at each location. The information which can be extracted from these images supports the earlier discussion of the histogram shapes and indicates the spatial homogeneity of the regional surface properties (which do not vary much in time) and of the temporal variability of cloudiness. To investigate the relations between these time statistics and the spatio-temporal statistics extracted from the time-cumulated histograms, radiance histograms have been built for these time-composite images in the same way as for the daily images (using 60×120 pixel regions). Generally these distributions have a very large peak (high regional homogeneity); thus we compare only the regional MOD values to the CUM parameters in table 7, which also give the percentage of pixels with values equal to the MOD value plus or minus a certain amount. For the VIS IM-MAX and IR IM-MIN, the value of PEAK is often small; therefore, we only report in table 7 the percentage of pixels colder or brighter than a certain value. We examine the spatial variability in these images by calculating the differences of the quantities as a function of separation distance, as for the original daily radiance images, and the SD of the MOD radiances.

7.1. *Time-composite images*

VIS IM-MIN and IR IM-MAX (figures 12(*a*) and (*b*)) are the darkest and warmest values attained at each location during the period and are commonly interpreted as clear sky radiances (cf. discussion by Rossow *et al.* 1985, 1989 b) with the VIS image controlled primarily by surface reflectance and the IR image by surface temperature. The regional homogeneity of the surface properties is apparent in these images. If clear conditions are encountered more than once during the time period, these values are generally biased darker and warmer than the average clear sky radiances (Sèze and Desbois 1987, Rossow *et al.* 1989 b). Note, however, that

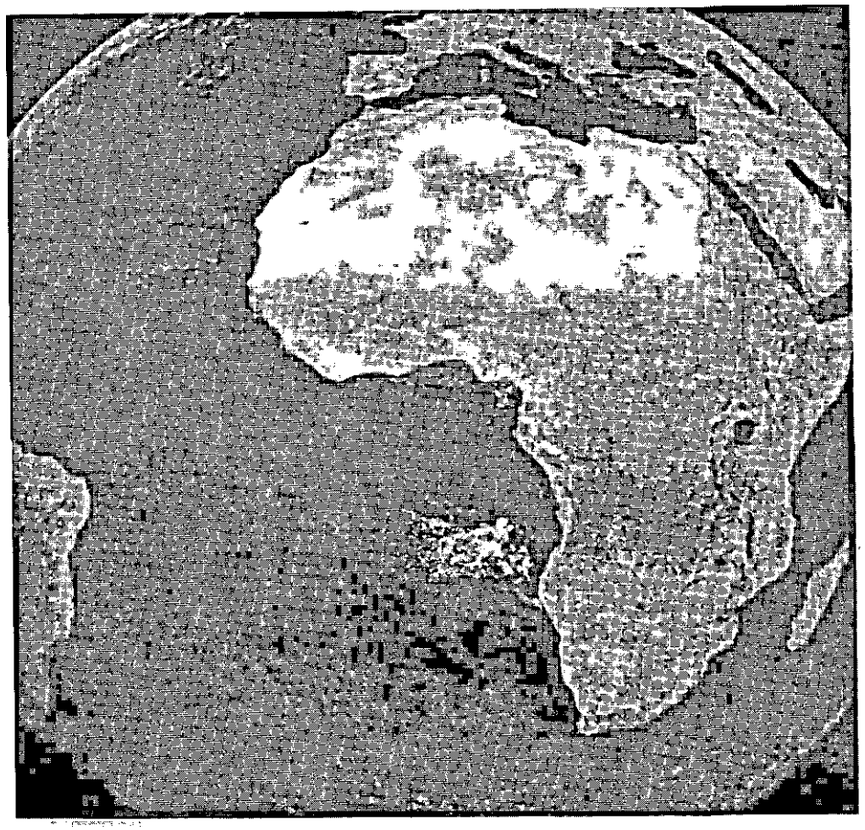

12 (*a*)

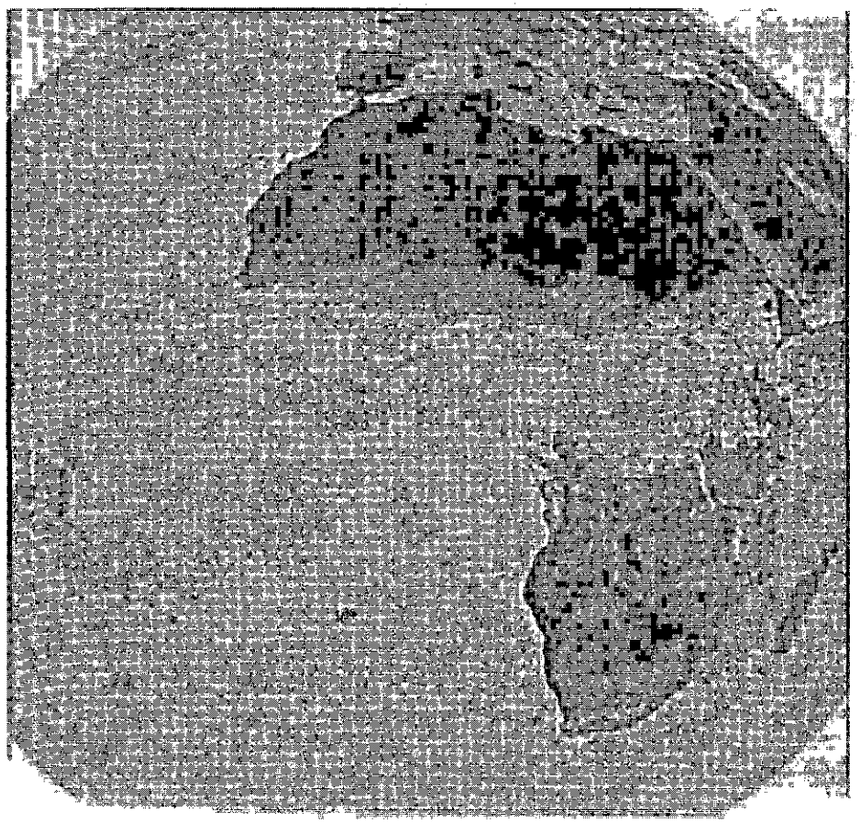

12 (*b*)

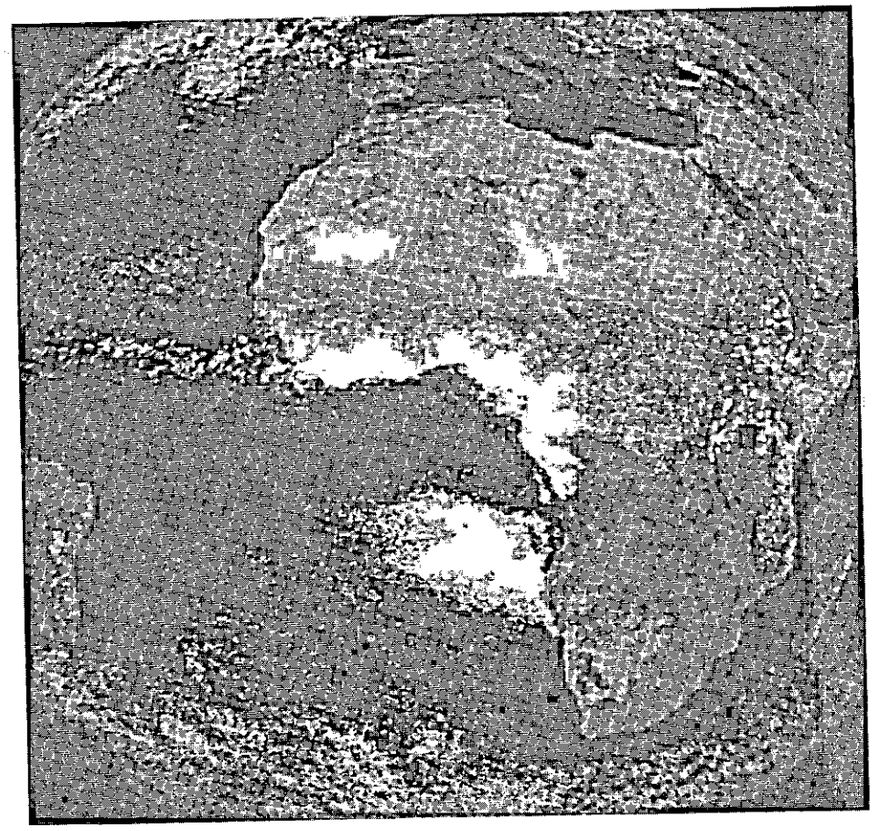

12(*c*)

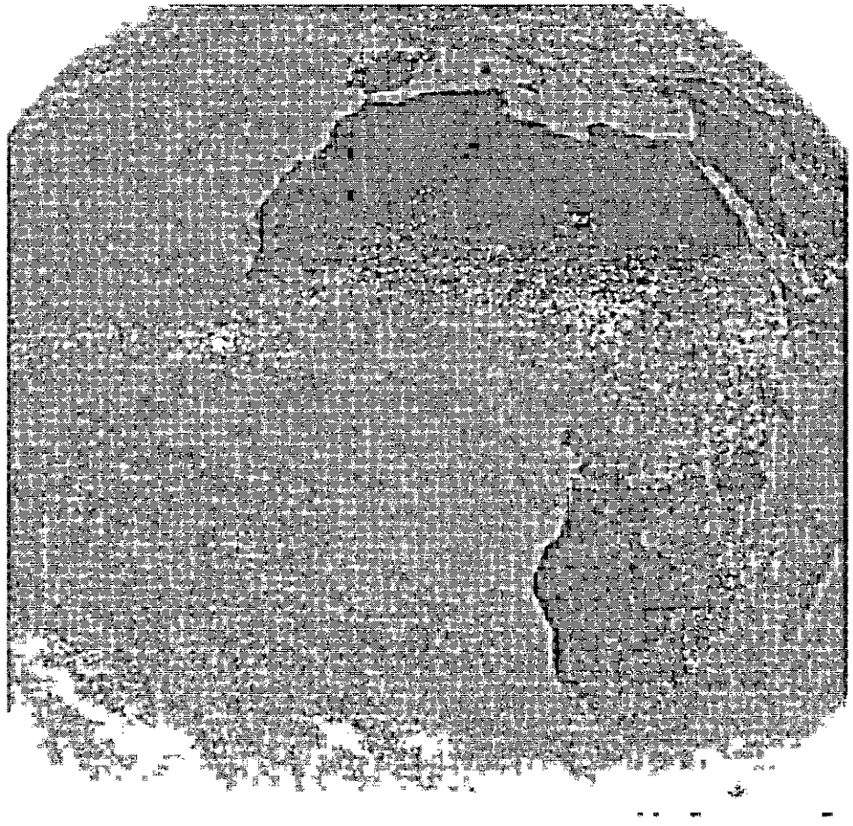

12(*d*)

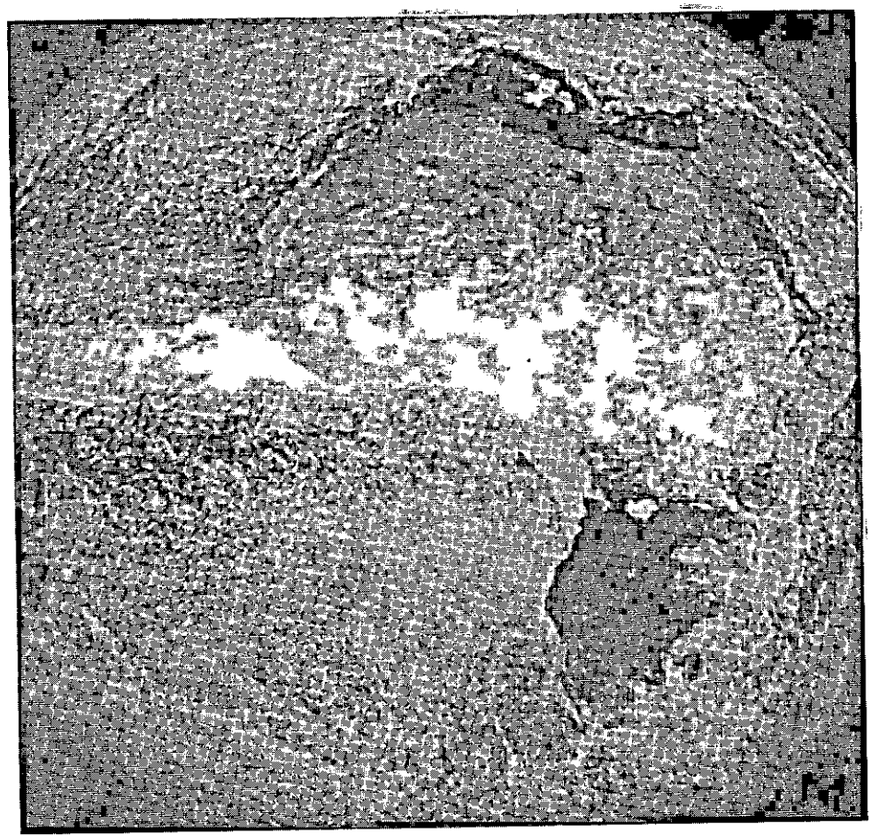

12 (*e*)

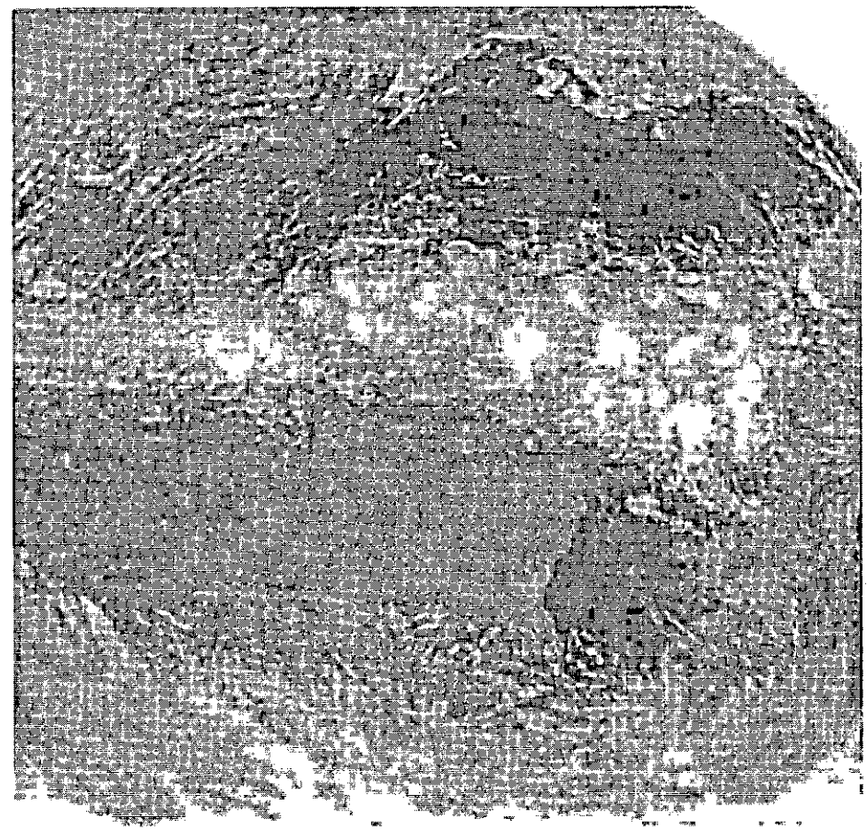

12 (*f*)

Figure 12. Time-composite images where the grey level at each location represents some statistics of the time series of radiances at that location over 17 days: (*a*) VIS MIN, (*b*) IR MAX, (*c*) VIS MOD, (*d*) IR MOD, (*e*) VIS MAX, and (*f*) IR MIN. The grey scale represents low values by darker shades and high values by lighter shades; low VIS counts represent dark scenes, while low IR counts represent warm scenes. The radiance values corresponding to a particular grey shade vary between images in order to show important details.

Table 7. CUM parameters (first line), the MOD of the IM parameters (second line), and the percentage of pixels with a radiance within a range, ±delta, of the MOD value for the seven regions (60 × 120 pixels). The parameters shown are the MIN, MAX, AVG and MOD. Delta values in VIS are 4 per cent for MIN, 8 per cent for MAX and 6 per cent for a AVG and MOD; in IR they are 3°C for MAX and 4°C for AVG and MOD. In the fourth line, the fraction of pixels in the IR IM-MIN image colder than some value or pixels in the VIS IM-MAX image brighter than some value are also reported. For IR the lowest values correspond to MAX temperatures and the highest values correspond to MIN temperatures.

	VIS				IR			
REGION	MIN	MAX	AVG	MOD	MAX	MIN	AVG	MOD
	64	172	90	92	23	201	42	38
N. AFR.	88	92	88	92	28	56	40	38
	92	94	99	96	95	—	98	98
					1·8% pixels colder than 160			
	72	204	95	96	18	203	71	78
SAHEL	92	104	96	96	46	168	78	80
	90	70	97	99	40	—	50	35
					25% pixels colder than 160			
	12	136	72	80	109	134	124	124
S. ATL.	12	108	68	80	114	128	124	125
	65	72	80	60	100	—	100	100
					94% pixels = MOD ± 1			
	8	220	64	16	100	232	144	108
TR. ATL.	12	188	68	16	102	220	146	108
	100	70	75	91	100	—	77	79
	85% pixels brighter than 150				94% pixels colder than 200			
	28	216	74	44	79	233	136	108
TR. AFR.	40	164	76	44	100	222	136	108
	99	54	92	91	85	—	87	71
	75% pixels brighter than 150				80% pixels colder than 200			
	16	212	79	48	69	221	132	96
EUROPE	44	148	76	48	86	200	130	96
	99	78	97	99	88	—	86	56
	77% pixels brighter than 150				93% pixels colder than 180			
	12	156	62	16	116	214	140	128
N. ATL.	16	112	56	16	120	182	140	126
	100	89	89	49	100	—	99	87
	99% pixels brighter than 100				90% pixels colder than 170			

over significant portions of the S. Atlantic area and parts of Tr. Africa, clear conditions were not found at all in the 17 day period.

VIS/IR IM-AVG (not shown): The radiance time averages associated with each location indicate the relative uniformity of mean (cloudy plus clear) conditions in a region, and have been used often in climatic studies (Hartmann and Short 1980, Cahalan *et al.* 1982, Desbois *et al.* 1988; Duvel 1988).

We next consider VIS/IR IM-MOD (figures 12(*c*) and (*d*)). The most frequent radiance values occurring at each location during the period are usually, but not always, representative of clear sky radiances, as demonstrated by the general

similarity of the MOD images to figures 12(*a*) and (*b*). This is caused by surfaces having lower time variability than clouds, allowing the clear radiances to form a peak in the distribution, even under quite cloudy conditions (see discussion in §4.2.3). Larger differences between the MOD images and figures 12(*a*) and (*b*) in some regions indicate the predominance of clouds. The spatial variations of the IM-MODs provide distinctive clues to the frequent presence of thin cirrus (high IR variance, low VIS variance) or low-level clouds (low IR variance, high VIS varianced) over a region.

VIS IM-MAX and IR IM-MIN (figures 12(*e*) and (*f*)) are formed by the brightest and the coldest radiances attained at each location; these values are related to two key characteristics of the cloud cover for the considered regions: the extreme water content and altitude for a cloud. These images show clearly the physical constraints, such as the altitude of the tropopause in the ITCZ or the height of the boundary layer in the S. Atlantic region. For the VIS, the constraint may be the saturation of the cloud reflectance with increasing water content. (The VIS MAX is also constrained by the maximum solar zenith angle that occurs during the time period, for example see Koepke and Kriebel (1987)). Especially noteworthy are the closeness of IR MIN and IR MAX in the moving status clouds in the S. Atlantic and the 'clustering' of convective activity over Africa (Desbois *et al.* 1988).

7.2. *Regional comparisons of CUM parameters and IM parameters*

The satial differences are smallest for the composite images VIS IM-MIN and IR IM-MAX. For a 70 pixel separation the average differences are ⩽4 per cent and 5°C; for a 5 pixel separation they are ⩽2 per cent and 1°C. The surface spatial variability in VIS is highest for the desert areas, but of the same order as for other land surfaces in IR. The near absence of cloud during the period over N. Africa makes the spatial differences in the VIS-MIN images very close to those of the original daily images. The bimodal distribution of surface temperatures in the Sahel explains the small percentages of locations with IM parameter values close to their MOD in table 7.

The land–sea contrast appears clearly in these images. Some of the large changes introduced in the radiance statistics and time-cumulated histograms by increasing the region size to include different surface conditions are related to the magnitude of this land–sea contrast. Differences are also found between the regional MOD of IR IM-MAX and the IR CUM-MAX, which indicate the magnitude of the spatial variability of land surface temperatures (Europe) and/or atmospheric conditions (Tr. Africa).

The low spatial variability of the surface reflectance and the usefulness of the VIS/IR CUM-MOD to represent the mean surface properties for a given region is confirmed by the similarity of the regional MOD of VIS IM-MIN and the VIS CUM-MOD.

The relationship between the two statistics VIS/IR IM-AVG and IM-MOD depends on the relative asymmetry of the VIS and IR radiance distributions (cf. figure 5), usually controlled by the amount and properties of the cloudiness. For example, comparison of these two images shows a significant change in cloudiness between the northern and the southern part of Europe, the southern part being less cloudy than the northern part. In general, the most frequent and average radiance values (CUM-MOD and CUM-AVG) for a region are nearly the same as the most

frequent values (IM-MOD and regional MOD of IM-AVG) over the same time period for a single location.

On small spatial scales (< 350 km), the variability of IM-MOD is larger than of IM-AVG, but its independence of scale is caused by a poor definition of the MOD value for the time distributions with only 17 or 20 values. Decreasing the radiance resolution would increase the spatial homogeneity of IM-MOD (see SR91); however, small changes in the spatial variability of IM-MOD can be a sensitive indicator of cirrus or low-level cloudiness. The spatial homogeneity of IM-AVG is high: for VIS IM-AVG, the largest difference is 6 per cent and for IM-AVG, it is 4°C for 70 pixel separations. However, the rate of increase of IM-AVG differences with separation distance is usually more rapid than for IM-MOD, since IM-AVG is more influenced by cloud spatial variations and IM-MOD is more influenced by surface spatial variations. The largest spatial variations in the VIS IM-MOD are found in the two regions of extensive and persistent cloudiness, the N. Atlantic and S. Atlantic. In these regions the MOD image is formed by a mixture of very dark radiances, representing clear ocean, and bright cloudy radiances.

In the multi-layered cloud regions the IM-MOD still generally represents surface properties. However, from the spatial variances of the VIS and IR MOD images in some places, we infer that parts of Europe and Tr. Africa are often covered by thin, middle or high clouds (indicated primarily by the IR variations) and that parts of the N. Atlantic and S. Atlantic are often covered by low-level clouds (indicated primarily by the VIS variations). For Tr. Atlantic both variances are high, but they are not correlated. This decoupling is caused by the frequent occurrence of two cloud types, cirrus and low-level clouds, in this region. In Tr. Africa the relatively high correlation (0·58) between the VIS IM-MIN and IR IM-MAX (too high to be attributed to surface variations), and the lack of correlation between the VIS IM-MOD and the IR IM-MOD, indicate the presence of persistent low broken clouds or a very high level of humidity and haze near the surface.

The two quantities VIS IM-MAX and IR IM-MIN are related to the spatial scales of the brightest and/or coldest parts of clouds; the differences increase quickly for spatial separations from 1 to 5 pixels and then more slowly for larger separation distances. Except for the desert regions in IR, the spatial differences are smaller in these images that in the original images; the high variability of the VIS IM-MAX and the warm value of the regional MOD of IR IM-MIN confirm the rarity of thicker cirrus or altostratus and the large variation in the properties of cirrus. In N. Africa the similarity of these quantities to their respective MOD values indicate that some pixels were never covered by clouds (or only by extremely thin cirrus or dust) during the period.

In the S. Atlantic the IR IM-MIN is remarkably uniform, again demonstrating the homogeneity of this layered cloud cover. The rare appearance of higher clouds shows up distinctly, however, as an occasional descrease in IR IM-MIN at some locations, which can lead to a large discrepancy between the IR IM-MIN and the IR CUM-MIN. The variability in the VIS IM-MAX (5 per cent for a 70 pixel distance separation) is smaller than in the ITCZ and Europe regions, but the large differences between the regional MOD of VIS IM-MAX and VIS CUM-MAX demonstrate that the spatial variability of 'thick' cloud reflectances is still quite high.

For the ITCZ and midlatitude regions, each location has been covered at least once by a relatively cold (high) cloud and at least once by a relatively bright (thick) cloud; at midlatitudes these two may not be the same cloud. The deep convective

cloud systems in the ITCZ exhibit more spatial variability of cloud properties at small scales in VIS than the high- and middle-level clouds at midlatitudes. The IR IM-MIN shows much less spatial variability than VIS IM-MAX in these highly cloudy regions and the differences between the regional MOD or IR IM-MIN and the CUM-MIN are not too large, caused by the presence of extensive cirrus and thicker anvil clouds associated with the thicker convective clouds (Houze 1977, Hahn *et al.* 1982, 1984, Warren *et al.* 1985, 1986, 1988, Redelsperger 1987).

8. Discussion

8.1. *Space/time variability*

Since very few regions are completely cloud-free or cloud-covered on time scales of one month, the warm/dark portion (VIS MIN, IR MAX) of the cumulated histogram is usually indicative of surface characteristics, while the cold/bright portion (VIS MAX, IR MIN) is indicative of clouds (at least at low and middle latitudes at these wavelengths). Thus, the behaviour of the histograms examined here suggests some general characteristics of surfaces and cloud.

The MOD in most histograms is associated with clear sky (Phulpin *et al.* 1983). This association, even when the cloud amount is relatively high (e.g. Tr. Atlantic), is caused by the generally lower time and space variability of the surface compared to clouds. Variability of clear radiances shows a tendency to be smaller in time than in space in VIS with an opposite tendency in IR. Ocean surfaces have very small space and time variability in both VIS and IR; thus, very infrequent occurrences of clear conditions over oceans can still control the mode values in the radiance histograms. The clear radiances over land are somewhat more variable in space than for oceans, especially in IR. The VIS and IR radiance variabilities are also characterized by low COR values.

The radiances associated with cloudy conditions are generally more variable than the clear values near the mode, producing an elongated distribution towards cold/bright radiance values. The VIS radiances for clouds are generally more variable than the IR because of the occurrence of clouds in layers (Coakley and Bretherton 1982). The layered cloud systems also seem to be relatively large scale, as shown by the smaller variation of temperature in space than in time. The elongation, usually inducing a fairly large value of VIS-IR COR, has characteristic shapes indicative of different types of clouds. Changing relations between the variability of cloud emissivity and optical thickness and/or variation of the cloud partial coverage from one pixel to another (Reynolds and Vonder Naar 1977, Platt 1983, Arking and Childs 1985) can produce both linear and non linear relationships in VIS–IR. In the case of a single cloud layer, the slope of the elongation is a function of the height of the cloud top (S. Atlantic). For multiple layers, several elongated structures can appear inside the histogram shape, with different slopes corresponding to the different cloud altitudes (Tr. Atlantic); the large spreading of radiances between these structures corresponds to variations in optical thickness and/or to pixels partially covered by different types of clouds. Use of average radiance values to represent the cloud properties is not adequate to describe these variations of cloud effects on radiaiton.

These results show clearly that the larger variations in surface and cloud properties occur at relatively larger spatial scales, greater than 100 km; spatial variability increases monotonically with scale. In contrast, the temporal radiance variability for single locations is already large for time scales of a few days and

seems nearly independent of the time scale (our analysis does not resolve the diurnal cycle and does not cover a long enough period of time to identify the predominant time scales, cf. Duvel 1988). In a region, the temporal variability is almost always larger than the spatial variability of pixel separation distances of less than 70 pixels (350 km). The stability of the histogram statistics with increasing region size (figures 3 and 9) and the spatial homogeneity of time-series statistics also show that the small-scale variabilities characteristic of the different surface and cloud-cover types in a climate regime are homogeneous over scales of about 500–2000 km (Cahalan *et al.* 1982). However, it must be noted that large and abrupt variations in surface properties can occur on very small scales; transitions of cloud characteristics can occur on scales as small as 100–500 km.

8.2. *Cloud/ no cloud detection strategies*

The effectiveness of three commonly used cloud algorithms can be evaluated from these results. The most common method searches either a spatial region or a time period to identify the VIS MIN and/or IR MAX, which is taken to represent clear conditions; clouds are identified by radiances that differ from the VIS MIN and/or IR MAX by some threshold amount (Arking 1964, Reynolds and Vonder Haar 1977). The daily histograms for regions of $2{\cdot}5° \times 5°$ shows that the VIS MIN and IR MAX are not always representative of clear sky radiances for the whole region. On some days the entire region is covered by clouds. On the other hand, if the surface properties are determined for each location by taking its VIS MIN and IR MAX over some time period, the S. Atlantic illustrates a case where, even after 20 days, the VIS MIN and IR MAX do not represent cloud-free conditions.

Even if the VIS MIN and IR MAX do represent clear conditions, the contrast between the cloudy and clear conditions can be so small that even a small threshold magnitude misses significant amounts of cloud (the S. Atlantic illustrates this situtation in the IR). N. Africa illustrates the opposite problem with this approach: although the VIS MIN and IR MAX are associated with clear conditions, the variability of the VIS and IR for clear conditions is large enough that small thresholds will misclassify some (darker/colder) parts of the surface as clouds. In particular, the variations of VIS caused by thin cirrrus at one pixel are sometimes smaller than the regional variations of VIS under clear conditions. Thus, while detection of broken or thin clouds that produce only small radiance changes requires high sensitivity (i.e. small thresholds), the regional and temporal changes in the magnitude of clear scene radiance variations can lead to mistaken identifications.

If the purpose of the analysis is to describe the mean regional properties of the surface, then using the regional MOD or IR IM-MAX (cf. table 7) introduces a bias in the inferred surface properties. For analysis of surface properties at small spatial scales (pixel), use of the VIS IM-MIN and IR IM-MAX can also lead to significant biases for certain locations (Sèze and Desbois 1987). Although the VIS/IR IM-MODS values are usually not too far from VIS IM-MIN/IR IM-MAX and the CUM-MODs are not too far from the VIS CUM-MIN/IR CUM-MAX (because of the small surface variability), the magnitude of the separation varies with, but seems characteristic of, different surface types (Rossow *et al.* 1989a).

Other analysis methods classify the satellite images on the basis of the spatial variability of the radiances (Bunting and Fournier 1980, Coakley and Bretherton 1982, Desbois and Séze 1984b, Tsonis 1984): low variability is often taken to

represent clear conditions or completely overcast conditions. Comparison of the spatial variations exhibited in N. Africa and the S. Atlantic shows that there is no absolute amount of variation that distinguishes clear from cloudy conditions, just as there are not absolute radiance values that separate these two conditions. Although not as crucial as in the threshold methods, the problem of a distinct separation between surface and cloud properties remains (Rossow *et al.* 1985). Some new methods use the time variations rather than the spatial variations (Rossow *et al.* 1985), but similar difficulties arise.

A third type of method uses either of the techniques discussed above to identify clear and cloudy scenes, but then employs the differences in the radiance values representing clear and completely overcast conditions to scale intermediate radiance values in terms of fractional cloud cover (Coakley and Baldwin 1984, Arking and Childs 1985, Chow *et al.* 1986). This requires the assumption that some specific value of the radiances corresponds uniquely to overcast conditions and that fractional coverage is the primary cause of radiance variability. The daily variability of the histogram shapes shows the difficulty with the first assumption (figure 6). Although use of cumulated statistics over large enough regions or time periods could provide a better estimate (the MIN and MAX values attain their extremum values more quickly as the region size or the time period increases), in some regions (e.g. N. Africa and Sahel) no radiances corresponding to high and thick clouds occur, even after cumulation over long time periods.

Another difficulty is that when a large portion of the pixels have radiances close to the clear sky values (figures 4 and 5), the same VIS/IR radiance pair can correspond to very different cloud layers (Desbois and Sèze 1984a). We have also found that the VIS IM-MIN/IR IM-MAX and VIS IM-MAX/IR IM-MIN are not always correlated (i.e. a mixture of surface and cloud types in a single region can negate the simple correlation of the radiance variations with cloud-cover fraction). The nonlinear distributions of VIS/IR variations also argue against a single cause for them. This lack of linear correlation can also mean that the spatially averaged radiances, if calculated separately for each spectral band, may not correspond to the actual clouds that occurred in the region.

8.3. *Description of the climate*

The time and space evolution of the histogram statistics shows rapid convergence to a long-term regional shape; our results provide quantitative confirmation of the idea that these long-term regional shapes are characteristic of specific climate regimes (figure 3), defined by the surface and cloud types that can be described by the histograms themselves. This statistical characteristic is relatively stable for spatial scales from 300 up to about 2000 km and time scales from 5 days up to a month. That the shape (and quantitative statistics) of the histograms is constant over large regions with abrupt transitions to different shapes, whereas the 'statistic' of variation at small scales is relatively uniform over smaller scales, suggests a fundamental difference in the nature of the radiance (cloud property) variations controlled by smaller and larger scale atmospheric motions (Gifford 1989, Cahalan and Joseph 1989). The comparison of the 'summer' and 'winter' patterns (figure 3) also shows that the boundaries between the cloud-type regimes are seasonally variable, in addition to their complicated geographical distribution. Interpretation of these shapes in terms of physical cloud properties and the control of their variability by atmospheric motions has to be developed further.

The time-composite images (figure 12) represented for a specific region some of the main characteristics of the surface and the cloud cover for the considered period (e.g. they provide some indications of the spatial and temporal variability of the surface properties, of the frequency of occurrence of clouds over the region, and of the main characteristics of the most common cloud types that occur). To test the spatial homogeneity of surface properties and mean cloud properties, visible minimum, infrared maximum, and visible and infrarted average time-composite images can be used to select homogeneous regions.

We have illustrated some of the features of the main climate regimes. The sub-tropical land areas (deserts) are almost always clear and are revealed as warm and bright regions in the VIS IM-MIN/IR IM-MAX, VIS/IR IM-MOD, and VIS/IR IM-AVG images. The uniform shape of the radiance histograms for these areas suggests that the most common cloud types in these areas are cirrus and altostratus (Warren *et al.* 1986). The sub-tropical oceans are either nearly cloud-free (in their western parts, not studied here) or almost completely covered by persistent low-level clouds (Warren *et al.* 1988), as shown by the broad distribution of VIS and narrow distribution of IR radiances. The multi-layered regions (the ITCZ and midlatitudes) are clearly defined as regions with very bright and cold areas in the VIS IM-MAX and IR IM-MIN and relatively bright and cold areas in the IM-AVG (figure 12). The frequency of cloud occurrence above these regions is revealed by the VIS/IR IM-MODs and their spatial variability. The variations of VIS/IR IM-AVGs, the IR IM-MIN and the VIS IM-MAX demonstrate the variability in the percentage of high cloud cover within the ITCZ. The differences in the morphology (spatial scale) of the high clouds between the ITCZ and the midlatitude cloud systems also appears clearly in the IR IM-MIN and VIS IM-MAX images. Although the magnitude of the variability of clouds seems similar in the tropics and midlatitudes, the time and space variations are comparable in the tropics, whereas in midlatitudes over land the time variations are larger than the spatial variations. Another difference between the tropics and the midlatitudes is that in the tropics the coldest clouds also correspond to the brightest clouds; this is not always the case in midlatitudes.

The maximum temperature in the ITCZ (IR IM-MAX) is similar for land and ocean. Over the ocean this temperature seems more closely related to the actual surface temperature, although the correction for atmospheric absorption is large in this area due to high absolute humidity (Rossow *et al.* 1989a). Over the land the occasional large value of VIS IM-MIN and the uniformity of the IR IM-MAX suggests the presence of a persistent low-level cloud layer along the coast of the Gulf of Guinea and a low-level haze or broken cloud and high humidity layer in central tropical Africa. These conditions make an accurate determination of surface temperature very difficult.

8.4. *Conclusions*

Use of larger region sizes for radiance cumulation can reduce the time-cumulation period needed to obtain a good approximation of the 'climatological' radiance distributions, because the temporal radiance statistics are independent of location over large regions (associated with the generally uniform appearance of the time-composite images). As region size increases, the radiances attained on a certain day are more comparable to the cumulated radiance distribution for that region, as suggested by the convergence of AVG-SD and AVG-AREA to CUM-SD and CUM-AREA and the decrease of SD-SD. The extreme radiances are also closer to

those of the cumulated distributions, since the probability of having both cloudy and clear conditions together in the area at the same time is higher. In other words, the climatological distribution of radiances (time aggregation) is similar to the spatial distribution at any one time. These features confirm the usefulness of the time cumulated histograms and the time composited images for characterizing each climate regime.

For regions delineated as described in this paper, we have devised several good histogram shape indices and spatio-temporal radiance statistics that may provide a more compact description of the differences between adjacent climate regimes. Some are computed from the time comulated and daily radiance histograms: histogram surface area (CUM-AREA), 80 per cent CUM-AREA, 50 per cent CUM-AREA, number of 'peaks' and 'branches' in the shapes of these frequency distributions, VIS and IR MIN, MAX, MOD, SD, COR (correlation) of the time-cumulated distributions (CUM parameters), average and standard deviation of the same parameters for the daily histograms (AVG and SD parameters). Other statistics are computed from the radiance time series associated with each single pixel: MOD, SD and COR of the VIS and IR MIN, MAX, AVG, and MOD time-composite images (IM-MIN, IM-MAX, IM-AVG and IM-MOD).

For the surface properties, the comparison of the different spatio-temporal and temporal statistics (CUM parameters, AVG parameters and statistics obtained from the IM parameters), corresponding to the darkest and warmest radiances and to the most frequent radiances, provides an estimate of the mode and distribution of the surface radiances and the magnitude of their spatial and temporal variability. This comparison also determines whether the more frequent event is cloudiness or clear conditions. More generally, the comparison of the CUM and AVG parameters will allow separation of regions where time and space variations are comparable from regions where the space variability is smaller than the time variability.

For the cloud properties, the histogram surface areas separate multi-layer cloud-covered regions from regions characterized by one very frequent event (e.g. clear sky or stratocumulus cloud layer). For the multi-layer cloud covered regions, these quantities indicate the number of different types of events associated with the region for the time period (e.g. clear sky and thin or small broken cloud, high thick cloud, middle thick cloud, low thick cloud). The VIS and IR CUM-SD and the MOD time-composite image (IM-MOD) also separate the most common cloud types (e.g. cirrus, low cloud, high or middle cloud). The presence of rare events, such as cirrus or altostratus is indicated by comparing the coldest and brightest radiances (IR CUM-MIN/VIS CUM-MAX) with the average value of the daily histogram parameter (AVG-MIN/AVG-MAX) and the most frequent, coldest and brightest values for single pixels (VIS IM-MAX and IR IM-MIN). For regions characterized by relatively frequent occurrences of clouds (i.e. not deserts), the IR IM-MIN/VIS IM-MAX, VIS/IR MOD values, and the percentage of pixels colder or brighter than a certain value, characterize the coldest and brightest clouds. The correlation (COR) betwen these coldest and brightest values indicates whether the coldest cloud is generally the brightest cloud or not.

A key characteristic of these different indices and parameters is that they are almost indeendent of location within relatively large regions and stable over sufficiently long time scales, making them good descriptors of climate regimes. As we show in SR91, if the statistics are accumulated over time periods and region sizes of sufficient size to provide a large enough sample population (e.g. for the ISCCP

sampled resolution, a one month cumulation period over a region size of at least 500 km), they provide results that are comparable to those obtained from the full-resolution data set. This suggests the feasibility of developing a classification of the climate regimes based on these parameters, using just enough data to resolve the diurnal and seasonal time scales, in addition to the daily to synoptic time scales studied here.

Acknowledgments

This study was made possible by support from the NASA Climate Program (managed by Dr Robert A. Schiffer) for one of us (GS) to visit NASA Goddard Institute for Space Studies. We also benefited from conversations with colleagues; we thank M. Desbois, L. Garder, E. Matthews and I. Fung. Figures were drawn by L. Del Valle and final word-processing was done by E. Devine.

References

ARKING, A., 1964, Latitudinal distribution of cloud cover from TIROS III photographs. *Science*, **143**, 569–572.

ARKING, A., and CHILDS, J. D., 1985, Retrieval of cloud cover parameters from multispectral satellite measurements. *Journal of Climate and Applied Meteorology*, **24**, 322–333.

BUNTING, J. T., and FOURNIER, R. F., 1980, Tests of spectral cloud classification using DMSP fine mode satellite data. AFGL-TR-80-0181, Environmental Research Papers, 704, U.S. Air Force Geophysical Laboratory, Hanscom AFB, 42 pp.

CAHALAN, R. F., and JOSEPH, J. H., 1989, Fractal statistics of cloud field. *Monthly Weather Review*, **117**, 261–272.

CAHALAN, R. F., SHORT, D. A., and NORTH, G. R., 1982, Cloud fluctuation statistics. *Monthly Weather Review*, **110**, 26–43.

CHOU, M-D., CHILDS, J., and DORIAN, P., 1986, Cloud cover estimation using bispectral satellite measurements. *Journal of Climate and Applied Meteorology*, **25**, 1280–1292.

COAKLEY, J. A., and BALDWIN, D. G., 1984, Towards the objective analysis of clouds from satellite measurements. *Journal of Climate and Applied Meteorology*, **23**, 1065–1099.

COAKLEY, J. A., BERNSTEIN, R. L., and DURKEE, P. A., 1987, Effect of ship-track effluents on cloud reflectivity. *Science*, **237**, 1020–1022.

COAKLEY, J. A., and BRETHERTON, F. P., 1982, Cloud cover from high-resolution scanner data: detecting and allowing for partially filled fields of view. *Journal of Geophysical Research*, **87**, 4917–4932.

COULMANN, S., BAKAN, S., and HINZPETER, H., 1986, A cloud climatology for the south Atlantic derived from Meteosat 1 images. *Tellus* A, **38**, 453–461.

DEL GENIO, A. D., and YAO, M., 1987, Properties of deep convective clouds in the ISCCP pilot data set. Preprints, *Proceedings of the 17th Conference on Hurricanes and Tropical Meteorology*. (Miami: American Meteorological Society), pp. 133–136.

DESBOIS, M., and SÈZE, G., 1984a, Use of space and time sampling to produce representative satellite cloud classifications. *Annals of Geophysics*, **2**, 599–606.

DEBOIS, M., and SÈZE, G., 1984b, Application of the clustering method for the cloud cover analysis over tropical regions. ECMWF workshop on cloud cover parameterization in numerical models, November 1984. ECMWF report August 1985, pp. 263–283.

DESBOIS, M., KAYIRANGA, T., GNAMIEN, B., GUESSOUS, S., and PICON, L., 1988, Characterization of some elements of the Sahelian climate and their interannual variations for July 1983, 1984 and 1985 from the analysis of the METEOSAT ISCCP data. *Journal of Climate*, **1**, 867–904.

DESBOIS, M., SÈZE, G., and SZEJWACH, G., 1982, Automatic classification of clouds on METEOSAT imagery: Application to high-level clouds. *Journal of Applied Meteorology*, **21**, 401–412.

DUVEL, J. P., 1988, Analysis of the dirunal, interdiurnal and interannual variations during northern hemisphere summers using Meteosat Infrared channels. *Journal of Climate*, **1**, 471–484.

DUVEL, J. P., and KANDEL, R. S., 1985, Regional-scale diurnal variations of the outgoing infrared radiation observed by Meteosat. *Journal of Climate and Applied Meteorology*, **24**, 335–349.

GIFFORD, F. A., 1989, The shape of large trophospheric clouds, or "Very like a whale." *Bulletin of the American Meteorological Society*, **70**, 468–475.

HAHN, C. J., WARREN, S. G., LONDON, J., CHERVIN, R. M., and JENNE, R. L., 1982, *Atlas of Simultaneous Occurrence of Different Cloud Typers over the Ocean*. NCAR/TN−201+STR (Boulder, Colo: National Center for Atmospheric Research) 212 pp.

HAHN, C. J., WARREN, S. G., LONDON, J., CHERVIN, R. M., and JENNE, R. L., 1984, *Atlas of Simultaneous Occurrence of Different Cloud Types over Land*. NCAR/TN−241+STR (Boulder, Colorado: National Center for Atmospheric Research), 21 pp. plus 188 maps.

HARTMANN, D. L., and SHORT, D. A., 1980, On the use of the earth radiation budget statistics for studies of clouds and climate. *Journal of Atmospheric Science*, **37**, 1233–1250.

HARTMANN, D. L., and RECKER, E. E., 1986, Diurnal variation of outgoing longwave radiation in the tropics. *Journal of Climate and Applied Meteorology*, **25**, 800–812.

HOUZE, R. A., 1977, Structure and dynamics of a topical squall line system observed during GATE. *Monthly Weather Review*, **105**, 1540–1567.

HUGHES, N. A., 1984, Global cloud climatologies: A historical review. *Journal of Climate and Applied Meteorology*, **23**, 724–751.

HUGHES, N., A., and HENDERSON-SELLERS, A., 1985, Global 3D-nephanalysis of total cloud amount: Climatology for 1979. *Journal of Climate and Applied Meteorology*, **24**, 669–686.

KOEPKE, P., and KRIEBEL, K. T., 1987, Improvements in the shortwave cloud-free radiative budget accuracy. Part I: Numerical study including surface anisotropy. *Journal of Climate and Applied Meteorology*, **26**, 374–345.

MATHERTON, G., 1977, La théorie des variables régionalisées et ses applications. *Cahier Centre Morphologie Mathématiqued*, **5**, (Fontainebleau: École Nationale Supérieur des Mines de Paris).

MATTHEWS, E., 1983, Global vegetation and land use: New high resolution data bases for climate studies. *Journal of Climate and Applied Meteorology*, **22**, 474–487.

MINNIS, P., and HARRISON, E. F., 1984, Diurnal variability of regional cloud and clear sky radiate parameters derived from GOES data. Part II: November 1978 cloud distributions. *Journal of Climate and Applied Meteorology*, **23**, 1012–1031.

PHULPIN, T., DERRIEN, M., and BRARD, A., 1983, A two-dimensional histogram procedure to analyze cloud cover from NOAA satellite high resolution imagery. *Journal of Climate and Applied Meteorology*, **22**, 1332–1345.

PLATT, C. M. R., 1983, On the bispectral method for cloud parameter determination from satellite VISSR data: separating broken cloud and semitransparent cloud. *Journal of Climate and Applied Meteorology*, **22**, 429–439.

REDELSPERGER, J. L., *Élaboration et Validation d'une Modèle Tridimensionnelle de Convection Profonde Atmosphérique: Application au Cas des Lignes de Grains Tropicales*. Thèse de Doctorat d'État, Université Pierre et Marie Curie, Paris.

REYNOLDS, D. W., and VONDER HAAR, T. H., 1977, A bi-spectral method for cloud parameter determination. *Monthly Weather Review*, **105**, 446–457.

ROSSOW, W. B., 1989, Measuring cloud properties from space: A review. *Journal of Climate*, **2**, 201–213.

ROSSOW, W. B., MOSHER, F., KINSELLA, E., ARKING, A., DESBOIS, M., HARRISON, E., MINNIS, P., RUPRECHT, E., SÈZE, G., SIMMER, C., and SMITH, E., 1985, ISCCP cloud algorithm intercomparison. *Journal of Climate and Applied Meteorology*, **24**, 877–903.

ROSSOW, W. B., BREST, C. L., and GARDER, L. C., 1989a, Global seasonal surface variations from satellite radiance measurements. *Journal of Climate*, **2**, 214–247.

ROSSOW, W. B., GARDER, L. C., and LACIS, A. A., 1989b, Global, seasonal cloud variations from satellite radiance measurements. Part I: Sensitivity of analysis. *Journal of Climate*, **2**, 419–458.

SAUNDERS, R. W., 1985, Monthly mean cloudiness observed from Meteosat-2. *Journal of Climate and Applied Meteorology*, **24**, 114–127.

SCHIFFER, R. A., and ROSSOW, W. B., 1983, The International Satellite Cloud Climatology Project (ISCCP): The first project of the World Climate Research Program. Bulletin of the American Meteorological Society, **64**, 779–784.

SCHIFFER, R. A., and ROSSOW, W. B., 1985, ISCCP global radiance data set: A new resource for climate research. *Bulletin of the American Meteorological Society*, **66**, 1498–1505.

SÈZE, G., and DESBOIS, M., 1987, Cloud cover analysis from satellite imagery using spatial and temporal characteristics of the data. *Journal of Climate and Applied Meteorology*, **26**, 287–303.

SÈZE, G., and ROSSOW, W. B., 1991, Effects of satellite data resolution on measuring the space/time variations of surfaces and clouds. *International Journal of Remote Sensing*, **12**, 921–952.

SHORT, D. A., and CAHALAN, R. F., 1983, Interannual variability of climatic noise in satellite-observed outgoing longwave radiation. *Monthly Weather Review*, **111**, 572–577.

SIMMER, C., RASCHKE, E., and RUPRECHT, E., 1982. A method for determination of cloud properties from two-dimensional histograms. *Annals of Meteorology*, **18**, 130–132.

STOWE, L. L., YEH, H. Y. M., ECK, T. E., WELLEMEYER, C. G., KYLE, H. L., and the NIMBUS-7 CLOUD DATA PROCESSING TEAM, 1989, NIMBUS-7 global cloud climatology. Part II: First year results. *Journal of Climate*, **2**, 671–709.

TSONIS, A. A., 1984, On the separability of various classes from GOES visible and infrared data. *Journal of Climate and Applied Meteorology*, **23**, 1393–1410.

WARREN, S. G., HAHN, C., and LONDON, J., 1985, Simultaneous occurrence of different cloud types. *Journal of Climate and Applied Meteorology*, **24**, 658–667.

WARREN, S. G., HAHN, C. J., LONDON, J., CHERVIN, R. M., and JENNE, R. L., 1986, *Global Distribution of Total Cloud Cover an Cloud Type Amounts over Land.* NCAR/TN−273+STR (Boulder, Colorado: National Center for Atmospheric Research), 20 pp. plus 200 maps.

WARREN, S. G., HAHN, C. J., LONDON, J., CHERVIN, R. M., and JENNE, R. L., 1988, *Global Distribution of Total Cloud Cover and Cloud Type Amounts over Ocean.* NCAR/TN−317+STR (Boulder, Colorado: National Center for Atmospheric Research), 42 pp. plus 170 maps.

WELCH, R. M., KUO, K. S., WIELICKI, B. A., SENGUPTA, S. K., and PARKER, L., 1988, Marine stratocumulus cloud fields off the coast of southern California observed using LANDSAT imagery. Part I: Structural characteristics. *Journal of Applied Meteorology*, **27**, 263–278.

WYLIE, D. P., and MENZEL, W. P., 1989, Two years of cloud cover statistics using VAS. *Journal of Climate*, **2**, 280–392.